

1 **Title: Hydrogen Sulfide (H<sub>2</sub>S)-Producing Oral Bacteria May Protect Against**  
2 **COVID-19**

3 **Authors and Affiliation**

4 Meghalbahen Vaishnani<sup>1</sup>, Anupama Modi<sup>1\*</sup>, Kshipra Chauhan<sup>1</sup>, Bhavin Parekh<sup>2\*</sup>,

5 <sup>1</sup>School of Applied Sciences and Technology, Gujarat Technological University, Gujarat, India.

6 <sup>2</sup>Department of Validation Indic Knowledge through Advanced Research, Gujarat University

7 **\*Corresponding author**

8 Dr. Bhavin Parekh\*

9 Research fellow,

10 Department of Validation Indic Knowledge through Advanced Research

11 Gujarat University

12 Gujarat -380009

13 Email: [bp2580@googlemail.com](mailto:bp2580@googlemail.com)

14 Phone: +9192656 52730

15

16 Dr. Anupama Modi\*

17 Assistant Professor

18 School of Applied Sciences and Technology

19 Gujarat Technological University

20 Gujarat -382424

21 Email: [anupamarmodi@gmail.com](mailto:anupamarmodi@gmail.com)

22 Phone:+91 97995 03950

23 **Abstract**

24 COVID-19 mortality rates have varied dramatically across the globe. Yet the reasons behind  
25 these disparities remain poorly understood. While recent research has linked gut microbes to  
26 these variations, the role of oral bacteria, a main port of entry for the coronavirus, remains  
27 unexplored. We investigated the relationship between oral microbiota and COVID-19 mortality  
28 rates across eight countries. Raw sequencing data of 16S rRNA regions from oral microbiota in  
29 244 healthy subjects from eight countries were obtained from public databases. We employed a  
30 generalized linear model (GLM) to predict COVID-19 mortality rates using oral microbiota  
31 composition. GLM revealed that high abundances of hydrogen sulfide (H<sub>2</sub>S)-producing bacteria,  
32 particularly Treponema, predicted low COVID-19 mortality rates with a markedly low p-value.  
33 Unsupervised clustering using a combination of LIGER and t-SNE yielded four oral microbiome  
34 "orotypes." Orotypes enriched in H<sub>2</sub>S-producing bacteria coincided with lower mortality rates,  
35 while orotypes harboring Haemophilus or Rothia were associated with increased vulnerability.  
36 To validate our findings, we analyzed influenza mortality data from the same countries,  
37 observing similar protective trends. Our findings suggest that oral bacteria-produced H<sub>2</sub>S may  
38 serve as a critical initial defense against SARS-CoV-2 infection. H<sub>2</sub>S from oral bacteria may  
39 prevent infection through antiviral activity, blocking ACE2 receptors, suppressing cytokines, and  
40 boosting antioxidants. This highlights the oral microbiome's role in COVID-19 outcomes and  
41 suggests new preventive and therapeutic strategies.

42 **Keywords :** COVID-19, Oral bacteria, COVID-19 mortality rates, Treponema,  
43 H<sub>2</sub>S

## 44 **Abbreviation**

45 COVID-19: Coronavirus disease 2019

46 SARS-CoV-2: Severe Acute Respiratory Syndrome Coronavirus 2

47 GLM: Generalized linear model

48 LIGER: Linked Inference of Genomic Experimental Relationships

49 H<sub>2</sub>S: Hydrogen sulfide

50 t-SNE: t-distributed Stochastic Neighbor Embedding

51 NCBI: National Center for Biotechnology Information

52 RNA: Ribonucleic Acid

53 DNA: Deoxyribonucleic acid

54 RSV: Respiratory syncytial virus

55 Nrf2: nuclear factor erythroid 2–related factor 2

## 56 **Introduction**

57 Why did COVID-19 hit some countries harder than others?[1]. This remains one of the  
58 pandemic's most perplexing questions—a critical piece of the puzzle for future pandemic  
59 preparedness [1] [2]. Conventional risk factors like age and comorbidities like diabetes and  
60 obesity fail to fully explain this aspect [2] [3]. Emerging research implicates the human  
61 microbiome as a potential arbiter of COVID-19 outcomes [3]. Researchers have shown that low  
62 levels of certain gut bacteria, such as *Collinsella*, predict high COVID-19 mortality rates.  
63 *Collinsella* produces ursodeoxycholate, which may prevent infection and mitigate acute  
64 respiratory distress syndrome by suppressing cytokine storm syndrome[3].

65 What about the oral microbiota—the second largest microbial community in the body [4],  
66 SARS-CoV-2's first contact point[5] and our frontline defense against respiratory  
67 viruses[6]?Exploring this overlooked aspect could further illuminate why some individuals  
68 succumb to the virus while others remain resilient[7]. Intrigued by this possibility, we  
69 hypothesize that dynamic interaction between the virus and specific oral microbiome may confer  
70 varying degrees of susceptibility or resilience to COVID-19 across populations.

71 To test this hypothesis, we analyzed the relationship between oral bacterial composition in 244  
72 healthy subjects from eight countries and their respective COVID-19 mortality rates. Our  
73 findings reveal a negative correlation between four H<sub>2</sub>S-producing genera and COVID-19  
74 mortality, suggesting a potential protective role for this oral commensal. To validate these  
75 findings, we further analyzed influenza mortality rates in the same countries, confirming similar  
76 protective trends and strengthening the generalizability of our results to respiratory viral  
77 infections.

## 78 **Materials and Methods**

### 79 **Dataset**

80 To investigate the potential association between oral microbiota composition and COVID-19  
81 mortality rates, this study utilized publicly available healthy oral microbiome datasets from the  
82 National Center for Biotechnology Information (NCBI). The analysis encompassed data from  
83 eight countries: the United States, Australia, Brazil, Italy, Sweden, Saudi Arabia, Egypt, and  
84 Russia. These datasets were selected based on their accessibility and comprehensive coverage,  
85 corresponding to accession numbers PRJNA606501, PRJNA384402, PRJNA256234,  
86 PRJNA267483, PRJNA598825, PRJNA227796, PRJNA292800, and PRJDB5153. COVID-19  
87 mortality data, quantified as cumulative deaths per million population as of February 9, 2021,  
88 were obtained from '<https://ourworldindata.org/>'. This timeframe was chosen to precede the  
89 widespread distribution of vaccines, thereby minimizing potential confounding effects of  
90 vaccination campaigns on mortality rates. To maintain the integrity and breadth of the analysis,  
91 no filtering criteria based on age or sex were applied to the datasets. This approach preserved a  
92 diverse and representative subject range, allowing for a more comprehensive examination of the  
93 potential relationship between oral microbiota and COVID-19 mortality across different  
94 populations.

### 95 **Taxonomic Analysis of oral microbiota**

96 To classify the oral microbiota, OmicsBox (version 3.0.29) developed by BioBam  
97 Bioinformatics, utilizing the Kraken2 tool, was employed. Kraken2 performs taxonomic  
98 classification by analyzing k-mers in DNA short reads and querying a comprehensive database  
99 of species-specific k-mer information. This approach allowed for thorough and detailed

100 taxonomic profiling, covering both metabarcoding (16S rRNA gene) and metagenomic  
101 sequencing reads, thus ensuring robust and accurate taxonomic identification.

## 102 **Generalized Linear Model (GLM) Analysis**

103 To investigate the relationship between oral microbiota composition and COVID-19 mortality,  
104 Generalized Linear Models (GLMs) were employed. The 15 most abundant genera served as  
105 predictors, with COVID-19 mortality as the outcome variable(Fig 1). Model selection was  
106 performed using Akaike Information Criterion (AIC), comparing Gaussian, Gamma, and Inverse  
107 Gaussian distributions. The optimal model (Gamma distribution) was used to identify significant  
108 associations between specific genera and mortality rates.

## 109 **LIGER-tSNE Analysis**

110 A combination of Linked Inference of Genomic Experimental Relationships (LIGER) and t-  
111 distributed stochastic neighbor embedding (t-SNE) was employed in our analysis to explore and  
112 visualize the complex oral microbiome structures across different populations (Fig 1). This  
113 LIGER-tSNE combination was found to be a powerful tool for dimensionality reduction and  
114 clustering, allowing subtle patterns in the oral microbiome data that might have been overlooked  
115 by traditional analysis methods to be discerned. This innovative approach, originally developed  
116 for single-cell RNA sequencing data, proved highly effective in identifying distinct oral  
117 microbiome orotypes and their relationship to COVID-19 mortality rates.

## 118 **Results**

### 119 **Generalized Linear Model (GLM) Analysis**

120 16S rRNA sequencing data from 244 healthy subjects across eight countries (Table 1) were  
121 analyzed to examine the effects of oral microbiota on COVID-19 mortality rates. Relative  
122 abundance analysis at the genus level (Fig 2) revealed *Streptococcus*, *Prevotella*, *Veillonella*,  
123 *Fusobacterium*, and *Haemophilus* as the most prevalent genera.

124 Using GLM, COVID-19 mortality rates were predicted with the 15 most abundant genera, with  
125 the Gamma distribution yielding the lowest AIC. GLM results (Fig 3) highlighted a marked  
126 negative predictive value of *Treponema* abundance for COVID-19 mortality rates ( $p < 0.001$ ).  
127 *Campylobacter*, *Gemella*, and *Selenomonas* also showed negative correlations, albeit less  
128 significant.

### 129 **Linked Inference of Genomic Experimental Relationships (LIGER) Analysis**

130 Non-negative matrix factorization via LIGER identified four distinct oral microbiome clusters,  
131 termed "orotypes" (Fig 4A). For every orotype, the mean relative abundances of the top 15  
132 genera are calculated in (S3 Table). The most abundant 5 genera in each orotype are given in  
133 Supplementary Table 1 (S2 Table).. orotype distribution varied across countries in relation to  
134 COVID-19 mortality rates (Fig 4B). High mortality countries (e.g., Italy, USA) predominantly  
135 exhibited orotypes 2 and 3, while low mortality countries (e.g., Australia, Russia) showed a  
136 higher prevalence of orotype 4 (Fig 4B). Countries with intermediate mortality rates displayed a  
137 mixed distribution. Analysis of COVID-19 mortality rates across orotypes (Fig 4C) revealed a  
138 decreasing trend from orotypes 1 to 4, although not statistically significant ( $p = 0.203$ ,

139 Jonckheere-Terpstra trend test, [Fig 4D](#)). Notably, *Treponema* relative abundance significantly  
140 increased from orotypes 1 to 4 ([Fig 4E](#);  $p = 0.033$ , Jonckheere-Terpstra trend test, [Fig 4F](#)).

#### 141 **Other Genera of Interest and Combined Analysis**

142 Analysis of *Campylobacter*, *Gemella*, and *Selenomonas* individually revealed no significant  
143 trends across orotypes ([Figs S1a-f](#)). However, combined analysis of *Treponema*, *Gemella*,  
144 *Campylobacter*, and *Selenomonas* demonstrated a highly significant increasing trend from  
145 orotypes 1 to 4 ( $p = 7.198e-05$ , Jonckheere-Terpstra trend test, [Figs S1g-h](#)), suggesting a  
146 potential synergistic effect of these bacteria.

#### 147 **Validation with Influenza Mortality Data**

148 To validate these findings, influenza mortality rates in these eight countries (taken from  
149 '<https://ourworldindata.org/>' (2019)) were analyzed, given the similarities between COVID-19  
150 and influenza as respiratory viral illnesses. The influenza mortality chart ([Fig S2](#)) demonstrates  
151 that orotype 4 is linked to lower mortality rates in influenza, mirroring the trends observed with  
152 COVID-19. This further substantiates the potential protective role of orotype 4-associated  
153 microbial composition in respiratory viral infections.



## 154 Discussion

155 This study uncovers a fascinating link between specific oral bacteria—*Treponema*, *Gemella*,  
156 *Campylobacter*, and *Selenomonas*—and lower COVID-19 mortality rates (Fig 3). The unifying  
157 characteristic of these bacteria is their production of hydrogen sulfide (H<sub>2</sub>S), a molecule now  
158 implicated as a pivotal protective agent against respiratory viral infections. Our data reveal a  
159 striking pattern in oral microbial communities. Those dominated by *Haemophilus* (orotype 1) or  
160 *Rothia* (orotype2) appear to be associated with increased vulnerability to SARS-CoV-2 (S2  
161 Table). In contrast, communities enriched with H<sub>2</sub>S-producing bacteria (orotypes 3 and 4) exhibit  
162 a protective effect.

163 This pattern echoes recent findings by Ren et al., who observed a similar association between  
164 *Gemella* and *Rothia* abundance in the upper respiratory tract of healthy individuals and COVID-  
165 19 patients, respectively. Wu et al. (2021) also reported significant microbiome alterations in  
166 COVID-19 patients, including elevated *Rothia mucilaginosa* levels in both oral and gut samples.  
167 Interestingly, this potential protective role of H<sub>2</sub>S aligns with previous research on gut  
168 microbiota, where *Collinsella*, another H<sub>2</sub>S-producing bacterium, was identified as a protective  
169 factor against COVID-19 [3] [8].

170 The H<sub>2</sub>S-producing capacity of the identified bacteria is notable. *Treponema* species, particularly  
171 *Treponema denticola*, are notable for their high H<sub>2</sub>S production capacity due to multiple  
172 cysteine-degrading enzymes, potentially explaining their strong negative correlation with  
173 COVID-19 mortality[9] [10].*Gemella* species such as *Gemella morbillorum*, while less studied  
174 in this context, has been identified as a H<sub>2</sub>S producer, albeit at lower rates compared to some

175 other oral bacteria[9]. Campylobacter species, particularly *C. rectus*, and *Selenomonas* thrive in  
176 anaerobic conditions and are known H<sub>2</sub>S producers[9].

177 But how exactly does H<sub>2</sub>S exert its protective effects? Its antiviral properties, previously  
178 demonstrated against other RNA viruses including influenza and respiratory syncytial virus  
179 (RSV) infections [11] [12], likely extend to SARS-CoV-2. These include direct antiviral  
180 activity[12], modulation of viral entry via ACE2 and TMPRSS2 receptors[13], (Fig 5) anti-  
181 inflammatory effects[12], prevention of cytokine storm[14], and enhancement of antioxidant  
182 defenses through the Nrf2 pathway [15] (Fig-5). Our findings are consistent with recent clinical  
183 observations showing higher serum H<sub>2</sub>S levels in COVID-19 pneumonia survivors [16],  
184 reinforcing its potential as both a prognostic marker and therapeutic target. Furthermore, the  
185 validation of our results using influenza mortality data strengthens the broader implications of  
186 our findings, suggesting that the protective effect of H<sub>2</sub>S producing bacteria extends beyond  
187 COVID-19 to other respiratory viral infections.

188 Despite our promising findings, our study has several limitations. The observational nature of  
189 this study precludes establishing causality. Reliance on existing datasets may introduce biases,  
190 and the precise mechanisms of H<sub>2</sub>S protection warrant further investigation. Additionally,  
191 individual variations in oral hygiene and diet could not be controlled. These limitations highlight  
192 the need for longitudinal studies, controlled experiments, and clinical trials.

193 In conclusion, our study identifies a novel association between H<sub>2</sub>S-producing oral bacteria and  
194 reduced COVID-19 mortality, underscoring the oral microbiome's potential role in modulating  
195 respiratory viral infection outcomes. This work paves the way for innovative approaches in the  
196 fight against respiratory viral diseases, including the exploration of H<sub>2</sub>S-based therapeutics and  
197 probiotics.

198 **Acknowledgement:** None

199 **Disclosure of interest:** No potential conflict was reported by the author(s)

200 **Funding:** None

201 **Authour Contribution**

202 BP conceptualized the study, performed data analysis, interpreted the data, and wrote the  
203 manuscript. MV conducted data analysis, participated in the creation of graphics, tables, and  
204 charts, and managed the submission process. AM reviewed, edited, and refined the manuscript,  
205 and coordinated the submission process. KC assisted with initial data collection efforts and  
206 offered input on the taxonomic analysis approach.

## 207 References

- 208 [1] A. Karlinsky and D. Kobak, “Tracking excess mortality across countries during the  
209 COVID-19 pandemic with the World Mortality Dataset,” *elife*, vol. 10, p. e69336, 2021.
- 210 [2] D. Chang, X. Chang, Y. He, and K. J. K. Tan, “The determinants of COVID-19 morbidity  
211 and mortality across countries,” *Scientific reports*, vol. 12, no. 1, p. 5888, 2022.
- 212 [3] M. Hirayama *et al.*, “Intestinal *Collinsella* may mitigate infection and exacerbation of  
213 COVID-19 by producing ursodeoxycholate,” *PLoS One*, vol. 16, no. 11, p. e0260451, 2021.
- 214 [4] M. Kilian *et al.*, “The oral microbiome—an update for oral healthcare professionals,” *British  
215 dental journal*, vol. 221, no. 10, pp. 657–666, 2016.
- 216 [5] A. Kusiak *et al.*, “COVID-19 manifestation in the oral cavity—a narrative literature review,”  
217 *Acta Otorhinolaryngologica Italica*, vol. 41, no. 5, p. 395, 2021.
- 218 [6] M. Ptasiewicz *et al.*, “Armed to the teeth—the oral mucosa immunity system and  
219 microbiota,” *International Journal of Molecular Sciences*, vol. 23, no. 2, p. 882, 2022.
- 220 [7] L. Tan *et al.*, “Potential interaction between the oral microbiota and COVID-19: a meta-  
221 analysis and bioinformatics prediction,” *Frontiers in Cellular and Infection Microbiology*,  
222 vol. 13, p. 1193340, 2023.
- 223 [8] K. E. Murros, “Hydrogen sulfide produced by gut bacteria may induce Parkinson’s  
224 disease,” *Cells*, vol. 11, no. 6, p. 978, 2022.
- 225 [9] S. Persson, M. Edlund, R. Claesson, and J. Carlsson, “The formation of hydrogen sulfide  
226 and methyl mercaptan by oral bacteria,” *Oral Microbiology and Immunology*, vol. 5, no. 4,  
227 pp. 195–201, Aug. 1990, doi: 10.1111/j.1399-302X.1990.tb00645.x.
- 228 [10] L. Phillips, L. Chu, and D. Kolodrubetz, “Multiple enzymes can make hydrogen sulfide  
229 from cysteine in *Treponema denticola*,” *Anaerobe*, vol. 64, p. 102231, 2020.
- 230 [11] N. Bazhanov, O. Escaffre, A. N. Freiberg, R. P. Garofalo, and A. Casola, “Broad-range  
231 antiviral activity of hydrogen sulfide against highly pathogenic RNA viruses,” *Scientific  
232 reports*, vol. 7, no. 1, p. 41029, 2017.
- 233 [12] V. Citi *et al.*, “Anti-inflammatory and antiviral roles of hydrogen sulfide: Rationale for  
234 considering H<sub>2</sub>S donors in COVID-19 therapy,” *British J Pharmacology*, vol. 177, no. 21,  
235 pp. 4931–4941, Nov. 2020, doi: 10.1111/bph.15230.
- 236 [13] G. Yang, “H<sub>2</sub>S as a potential defense against COVID-19?,” *American Journal of  
237 Physiology-Cell Physiology*, vol. 319, no. 2, pp. C244–C249, Aug. 2020, doi:  
238 10.1152/ajpcell.00187.2020.
- 239 [14] E. Magli *et al.*, “H<sub>2</sub>S donors and their use in medicinal chemistry,” *Biomolecules*, vol. 11,  
240 no. 12, p. 1899, 2021.
- 241 [15] A. R. Bourgonje *et al.*, “N-Acetylcysteine and Hydrogen Sulfide in Coronavirus Disease  
242 2019,” *Antioxidants & Redox Signaling*, vol. 35, no. 14, pp. 1207–1225, Nov. 2021, doi:  
243 10.1089/ars.2020.8247.
- 244 [16] Z. Ren *et al.*, “Alterations in the human oral and gut microbiomes and lipidomics in  
245 COVID-19,” *Gut*, vol. 70, no. 7, pp. 1253–1265, 2021.
- 246

247

248

249 **List of legend**

250 **Table legend**

251 **Table 1:** Eight 16S rRNA-seq datasets from eight countries and the mortality rates of COVID-  
252 19.

253 **Figure legend**

254 **Fig.:1** The methodology for this bioinformatics pipeline (a) Healthy oral microbiome data was  
255 obtained from the National Center for Biotechnology Information (NCBI). (b) This data was  
256 processed and analyzed using OmicsBox software. (c) The most abundant bacterial genera were  
257 identified. (d) COVID-19 mortality rate data from Our World in Data was incorporated (e) A  
258 statistical model (Generalized Linear Model) was used to analyze the relationship between the 15  
259 most abundant genera and COVID-19 mortality. (f) A specialized technique called LIGER,  
260 typically used for analyzing single-cell RNA sequencing data, was applied to classify the oral  
261 microbiota of 244 healthy individuals into four distinct groups, termed "orotypes".

262 **Fig 2:** Genera level abundance of health oral metagenomic

263 **Fig 3:** Plot of p-values of 15 genera in a generalized linear model (GLM) to predict the COVID-  
264 19 mortality rates.

265 **Fig 4** (a) Unsupervised clustering of oral microbiota in 244 healthy subjects in ten countries by  
266 LIGER generated 4 orotypes. Each subject is plotted with t-SNE and is color-coded by its  
267 orotype. (b) Fractions of orotypes 1 to 4 in eight countries. eight countries are sorted in  
268 descending order of the COVID-19 mortality rates per million, which are indicated in  
269 parentheses. (c) The t-SNE plot is color-coded by the COVID-19 mortality rates in eight

270 countries. (d) Mean and standard error of the COVID-19 mortality rates in orotypes 1 to 4.  $p =$   
271  $0.203$  by Jonckheere-Terpstra trend test. (e) The t-SNE plot is color-coded by the relative  
272 abundance of genus *Treponema*. (f) Mean and standard error of the relative abundance of  
273 genus *Treponema* in orotypes 1 to 4.  $P = 0.033$  by Jonckheere-Terpstra trend test.

274 **Fig 5:** Proposed mechanisms of oral bacteria-produced hydrogen sulfide (H<sub>2</sub>S) in protecting  
275 against SARS-CoV-2 infection. H<sub>2</sub>S, produced by oral bacteria including *Treponema*, *Gemella*,  
276 *Campylobacter*, and *Selenomonas*, exhibits multifaceted protective effects against SARS-CoV-2.  
277 These include: (a) Direct antiviral activity, (b) Modulation of viral entry by altering ACE2 and  
278 TMPRSS2 receptors, (c) Anti-inflammatory effects and prevention of cytokine storm, and (d)  
279 Enhancement of antioxidant defenses through the Nrf2 pathway. These mechanisms, previously  
280 observed in other RNA viral infections, likely contribute to the potential protective role of H<sub>2</sub>S-  
281 producing oral bacteria against severe COVID-19 outcomes.

282 **Tables:**

283 **Table 1: Eight 16S rRNA-seq datasets from Eight countries and the mortality rates of**  
284 **COVID-19.**

285

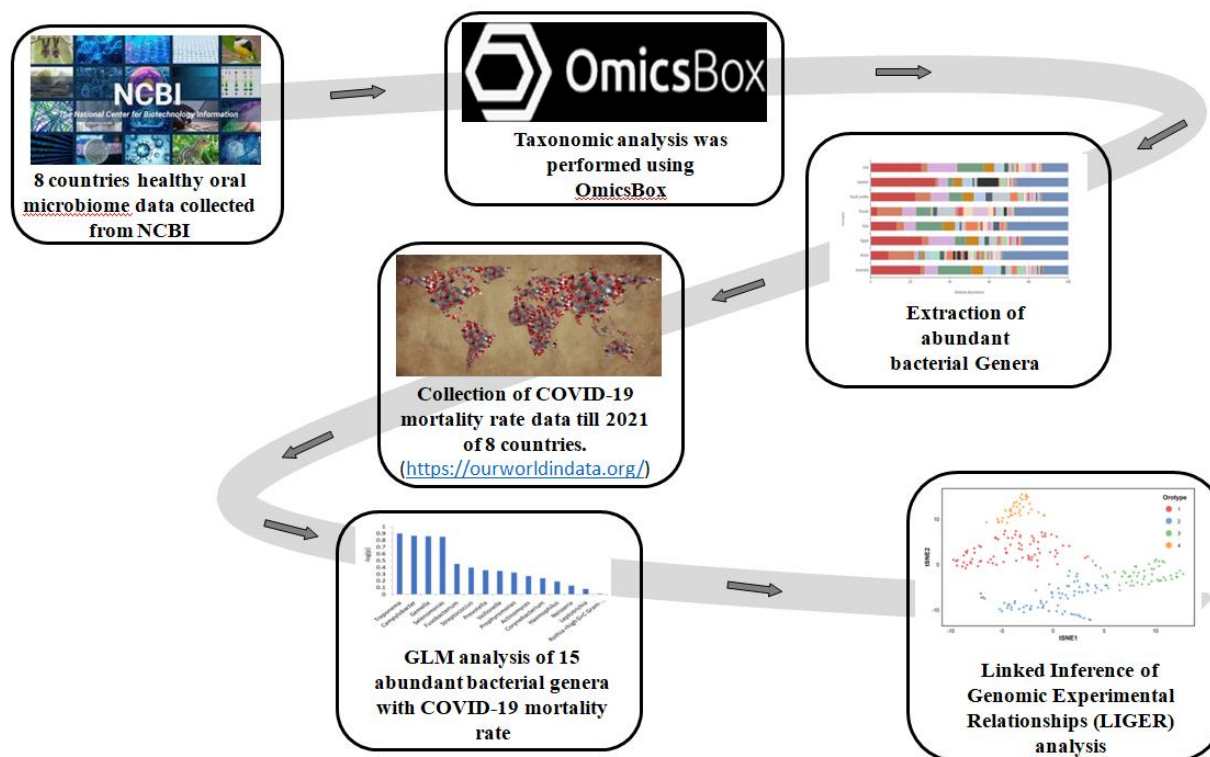
Dataset	City, Country	Accession number	Mortality rate per million <sup>a</sup>	The number of samples	Sequencing
1	Australia	PRJDB5153	35.26	18	16S rRNA (V3-V4)
2	Oklahoma, USA	PRJNA292800	1429.6	57	16S rRNA
3	Trento, Italy	PRJNA227796	1551.22	14	16S rRNA

<b>4</b>	Sweden	PRJNA598825	1188.41	12	16S rRNA (V3-V4)
<b>5</b>	Jazan, Saudi arabia	PRJNA267483	175.84	12	16S rRNA
<b>6</b>	Brazil, Sao Paolo, Piracicaba	PRJNA606501	1075.33	104	16S rRNA (V1-3 and V4-5)
<b>7</b>	Egypt	PRJNA384402	86.95	17	16S rRNA
<b>8</b>	Russia, Moscow	PRJNA256234	536.22	10	16S rRNA

286

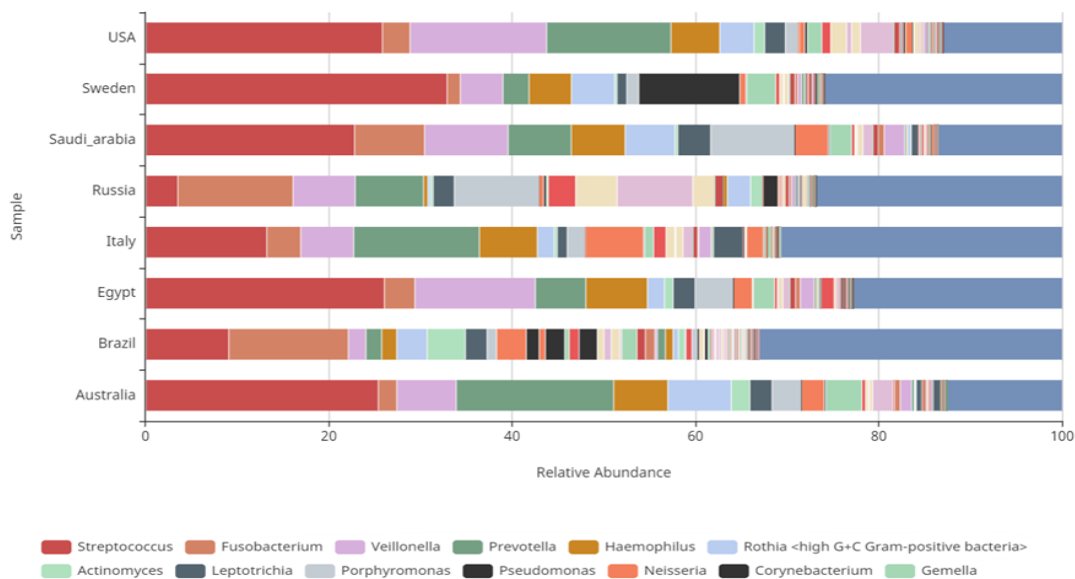
287

288 **Figures**



291 **Fig 1:** The methodology for this bioinformatics pipeline (a) Healthy oral microbiome data was  
292 obtained from the National Center for Biotechnology Information (NCBI). (b) This data was  
293 processed and analyzed using OmicsBox software. (c) The most abundant bacterial genera were  
294 identified. (d) COVID-19 mortality rate data from Our World in Data was incorporated (e) A  
295 statistical model (Generalized Linear Model) was used to analyze the relationship between the 15  
296 most abundant genera and COVID-19 mortality. (f) A specialized technique called LIGER,  
297 typically used for analyzing single-cell RNA sequencing data, was applied to classify the oral  
298 microbiota of 244 healthy individuals into four distinct groups, termed "orotypes".

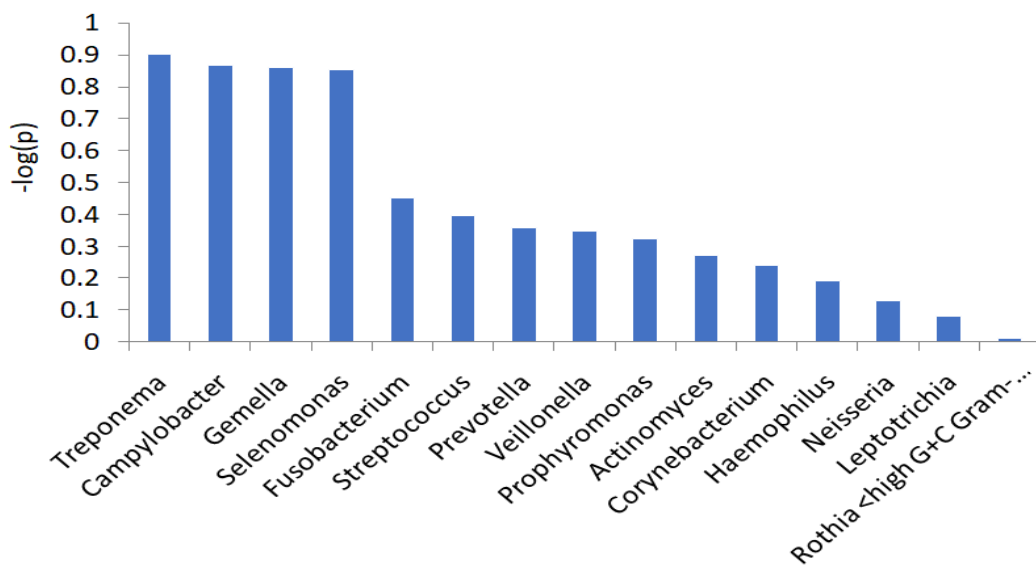




299

300

**Fig 2: Genera level abundance of health oral metagenomic**



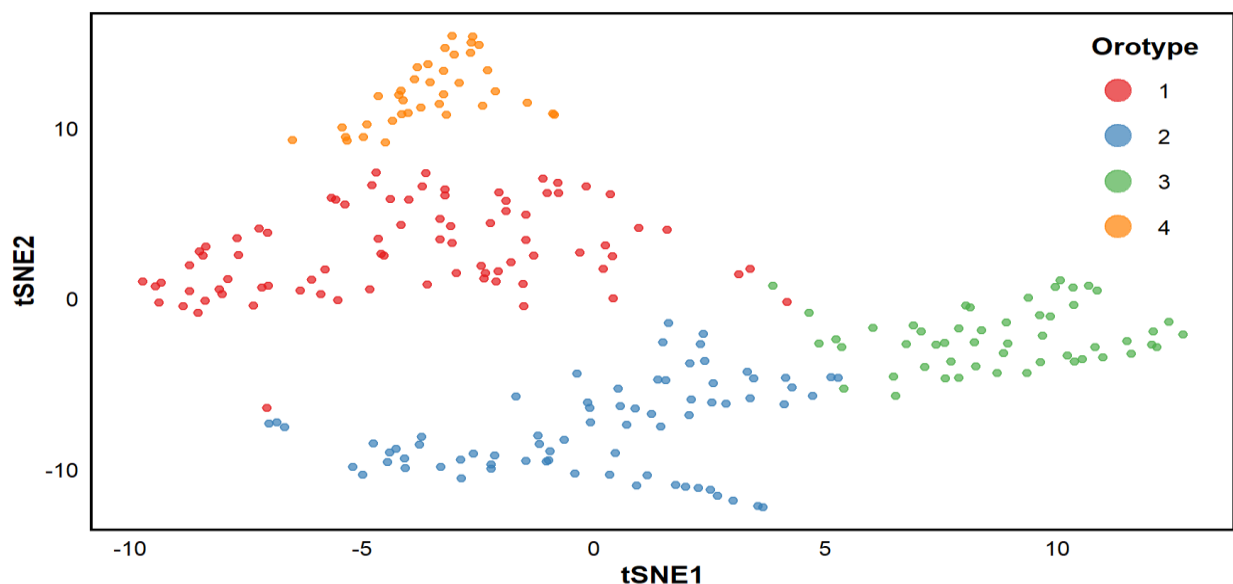
301

302

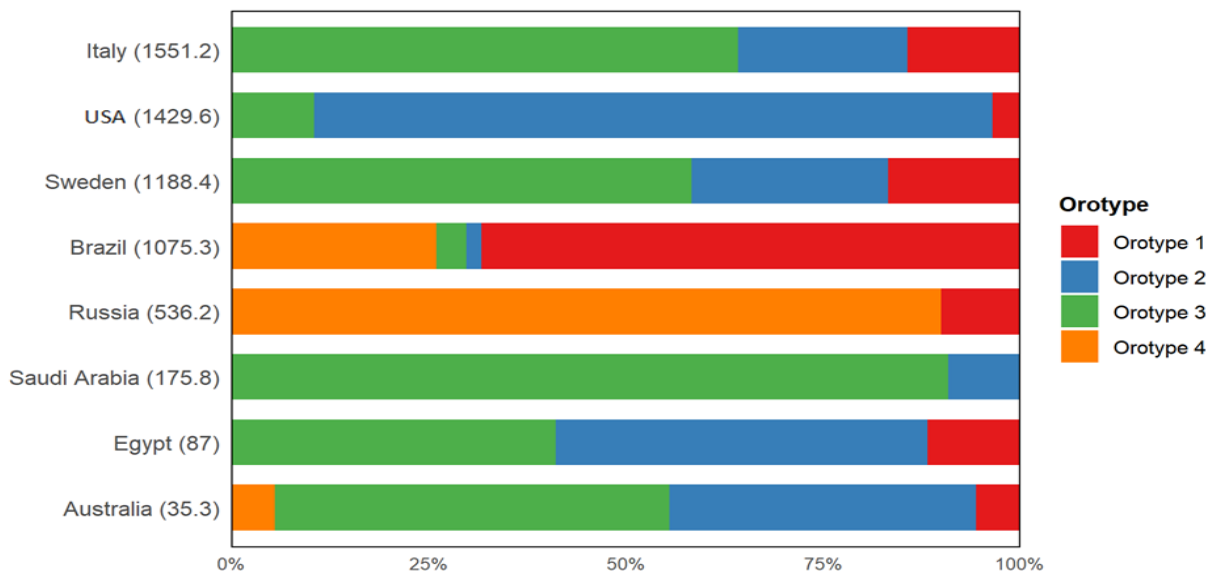
**Fig 3: Plot of p-values of 15 genera in a generalized linear model (GLM) to predict the COVID-19 mortality rates.**

304

305

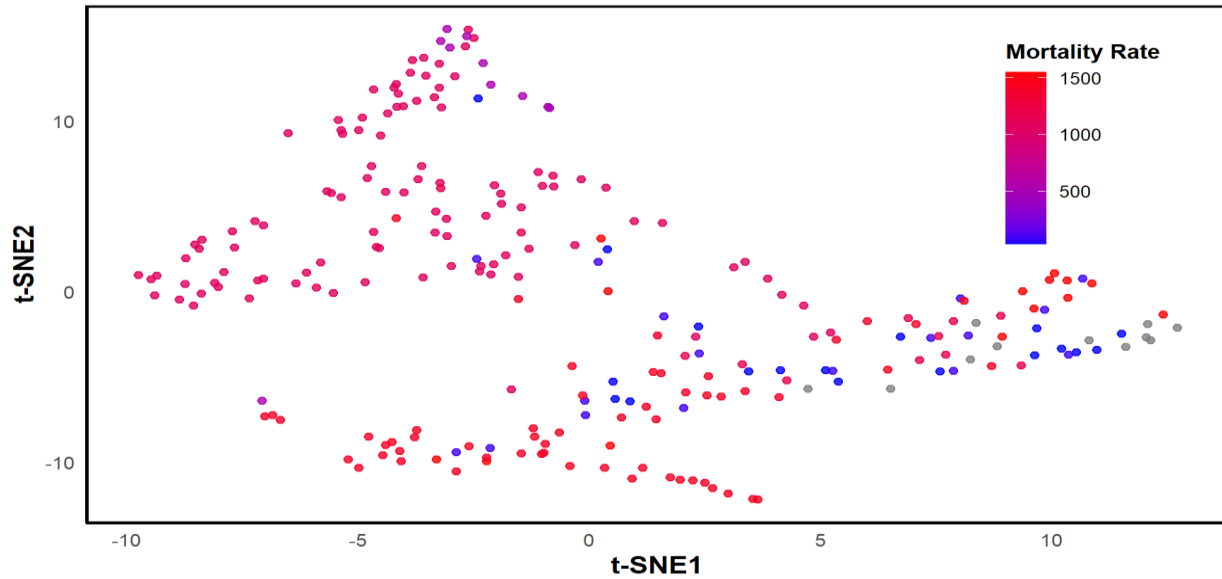


306  
307 **Fig 4 (a):**Unsupervised clustering of oral microbiota in 244 healthy subjects in ten countries  
308 **by LIGER generated 4 orotypes. Each subject is plotted with t-SNE and is color-coded by**  
309 **its orotype.**



310  
311 **Fig 4 (b):** Fractions of orotypes 1 to 4 in eight countries. eight countries are sorted in  
312 **descending order of the COVID-19 mortality rates per million, which are indicated in**  
313 **parentheses.**

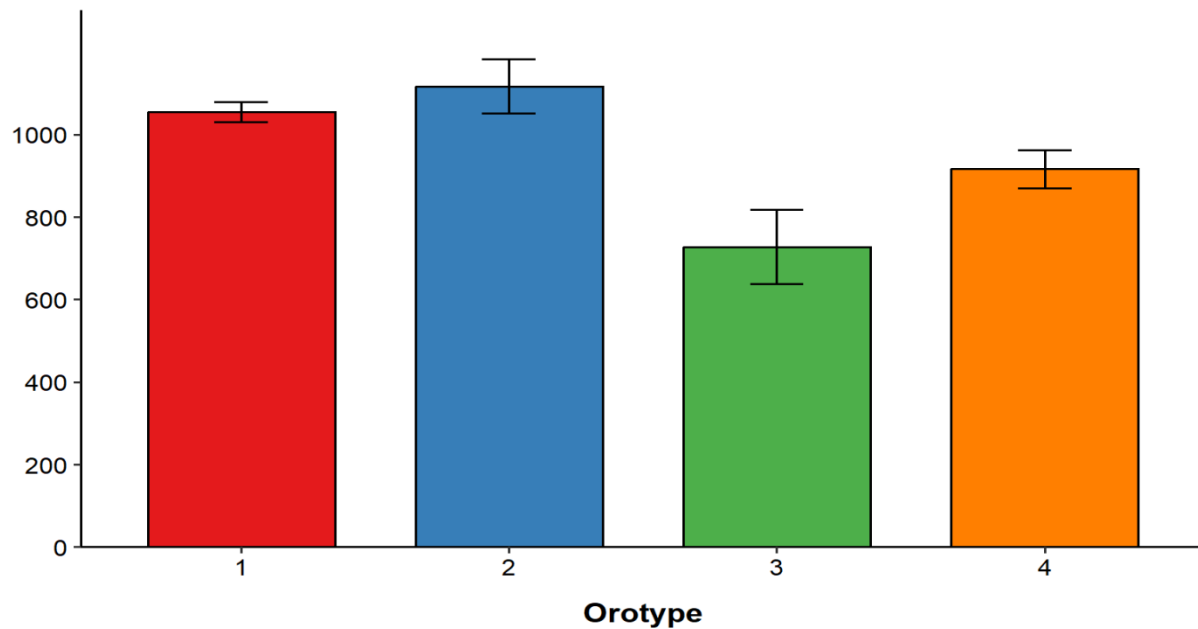
314



315

316 **Fig 4 (c): The t-SNE plot is color-coded by the COVID-19 mortality rates in eight**  
317 **countries.**

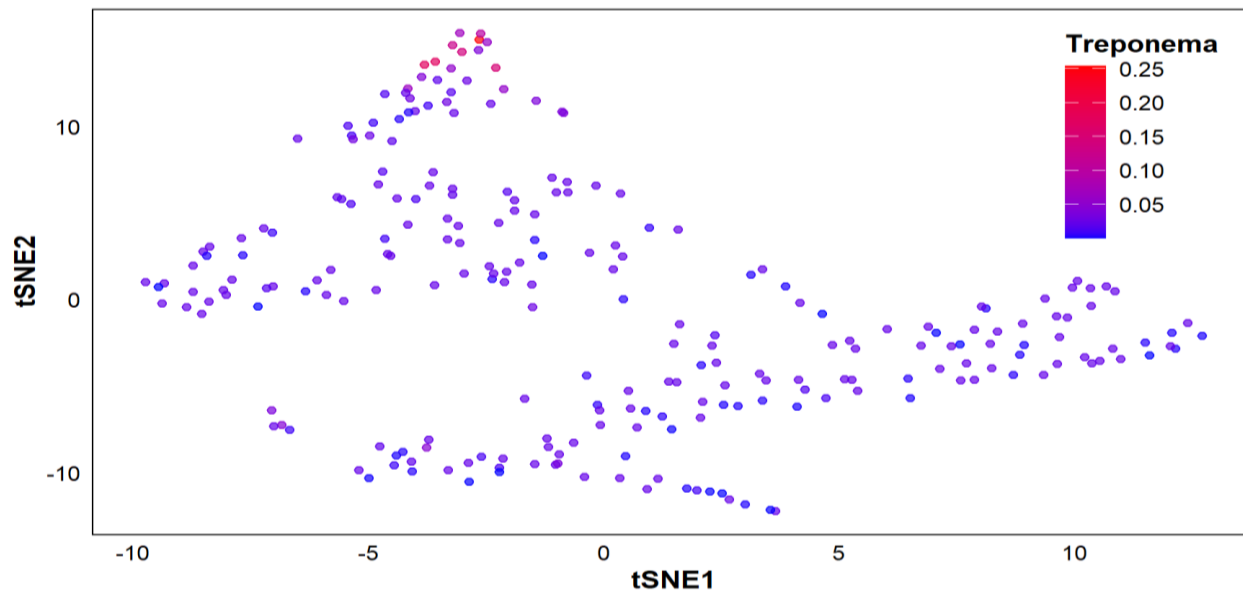
318



319

320 **Fig 4 (d): Mean and standard error of the COVID-19 mortality rates in orotypes 1 to 4.  $p =$**   
321  **$0.203$  by Jonckheere-Terpstra trend test.**

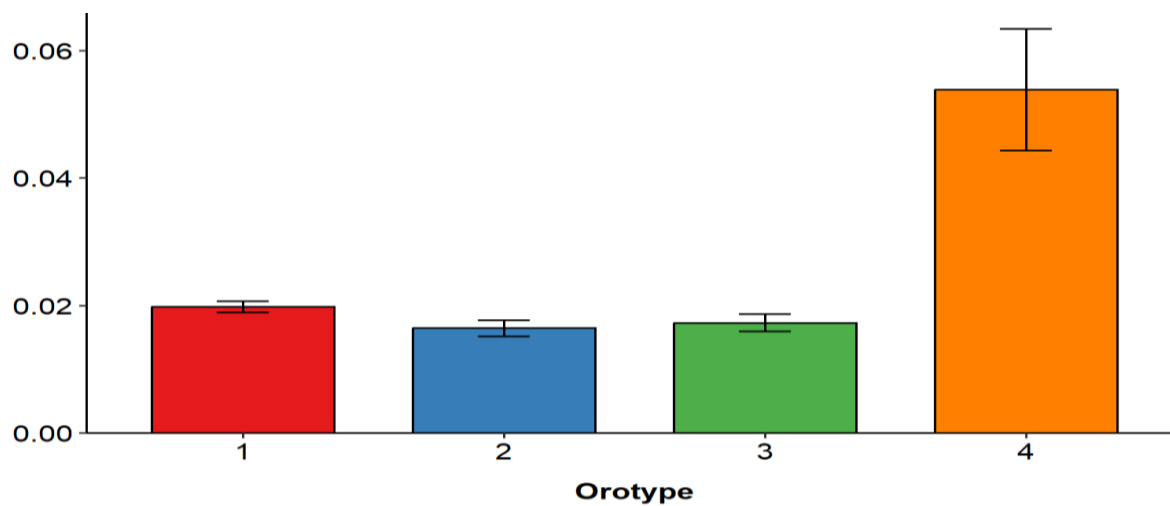
322



323

324

325 **Fig 4 (e):** The t-SNE plot is color-coded by the relative abundance of genus *Treponema*.



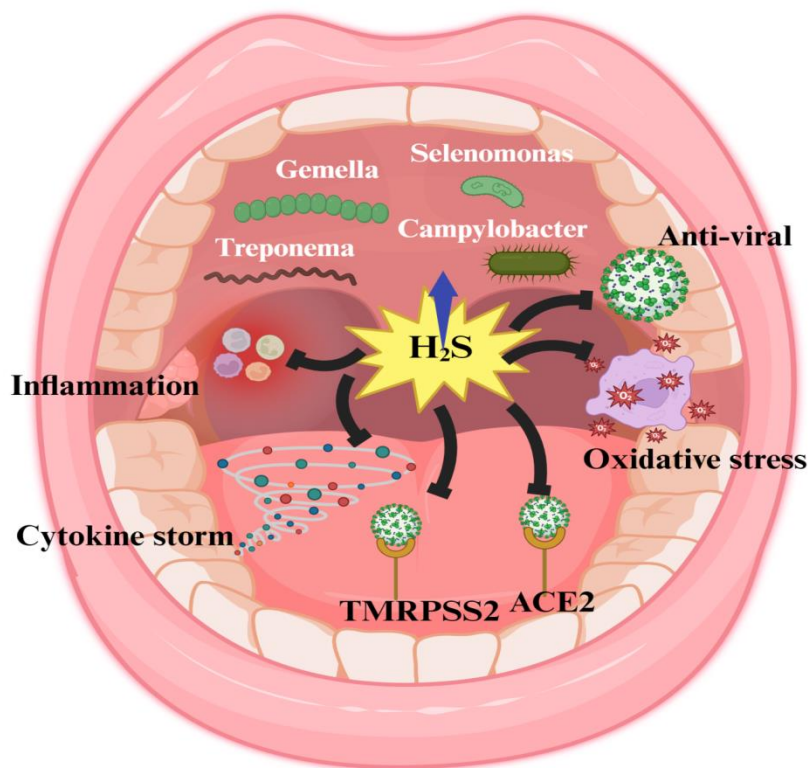
326

327

328 **Fig 4 (f):** Mean and standard error of the relative abundance of genus *Treponema* in  
329 orotypes 1 to 4.  $P = 0.033$  by Jonckheere-Terpstra trend test.

330

331



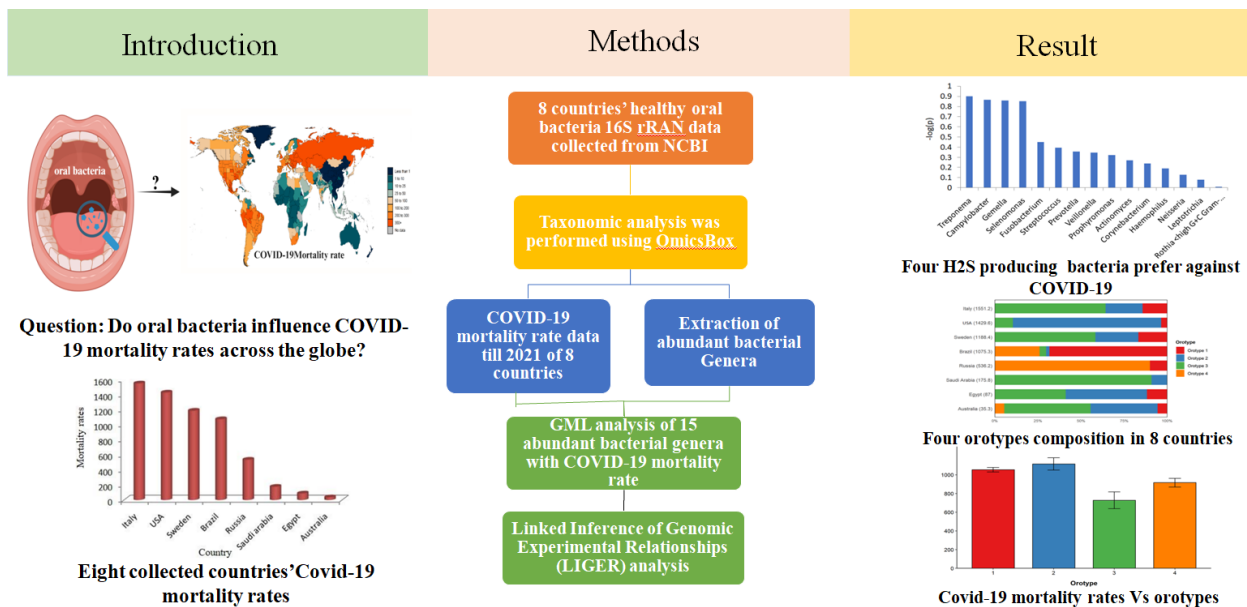
332

333

334 **Fig 5:** Proposed mechanisms of oral bacteria-produced hydrogen sulfide (H<sub>2</sub>S) in protecting  
335 against SARS-CoV-2 infection. H<sub>2</sub>S, produced by oral bacteria including Treponema, Gemella,  
336 Campylobacter, and Selenomonas, exhibits multifaceted protective effects against SARS-CoV-2.  
337 These include: (a) Direct antiviral activity, (b) Modulation of viral entry by altering ACE2 and  
338 TMRPSS2 receptors, (c) Anti-inflammatory effects and prevention of cytokine storm, and (d)  
339 Enhancement of antioxidant defenses through the Nrf2 pathway. These mechanisms, previously  
340 observed in other RNA viral infections, likely contribute to the potential protective role of H<sub>2</sub>S-  
341 producing oral bacteria against severe COVID-19 outcomes.

342

343 **Graphical Abstract**



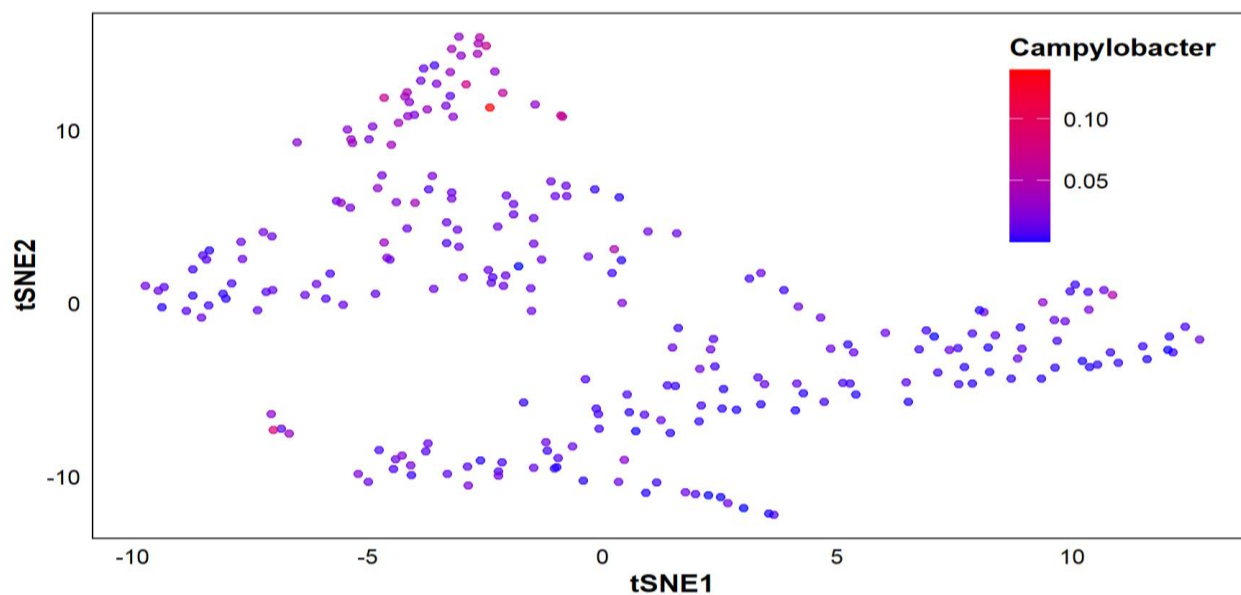
344

345

346

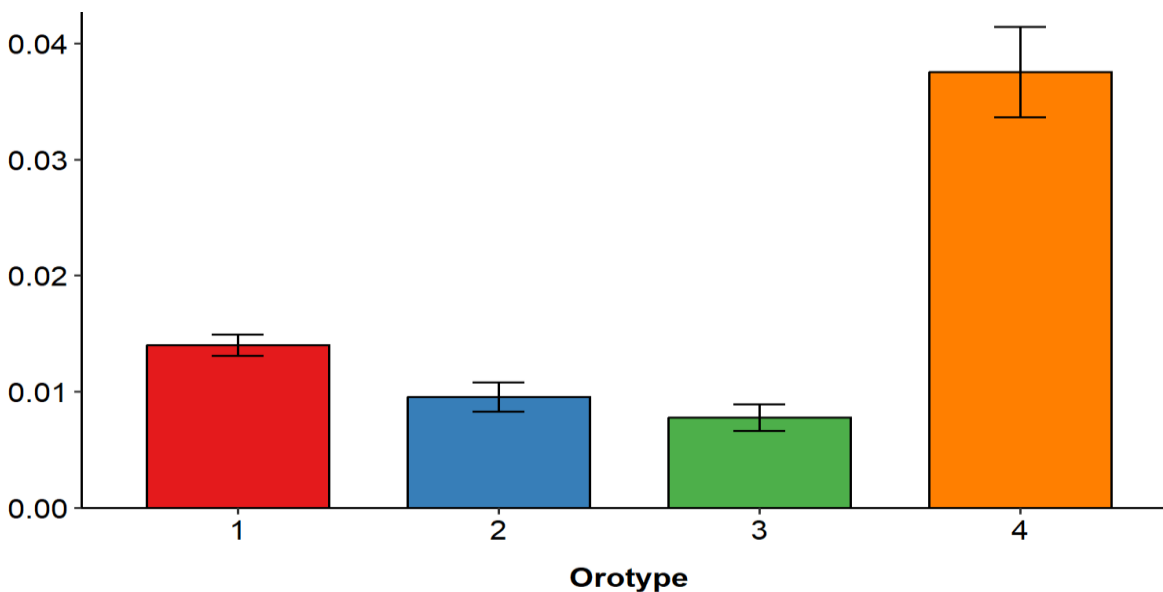
## Supplementary Information

347



348

349 **Fig S1a:** The t-SNE plot is color-coded by the relative abundance of  
350 *genus Campylobacter*.

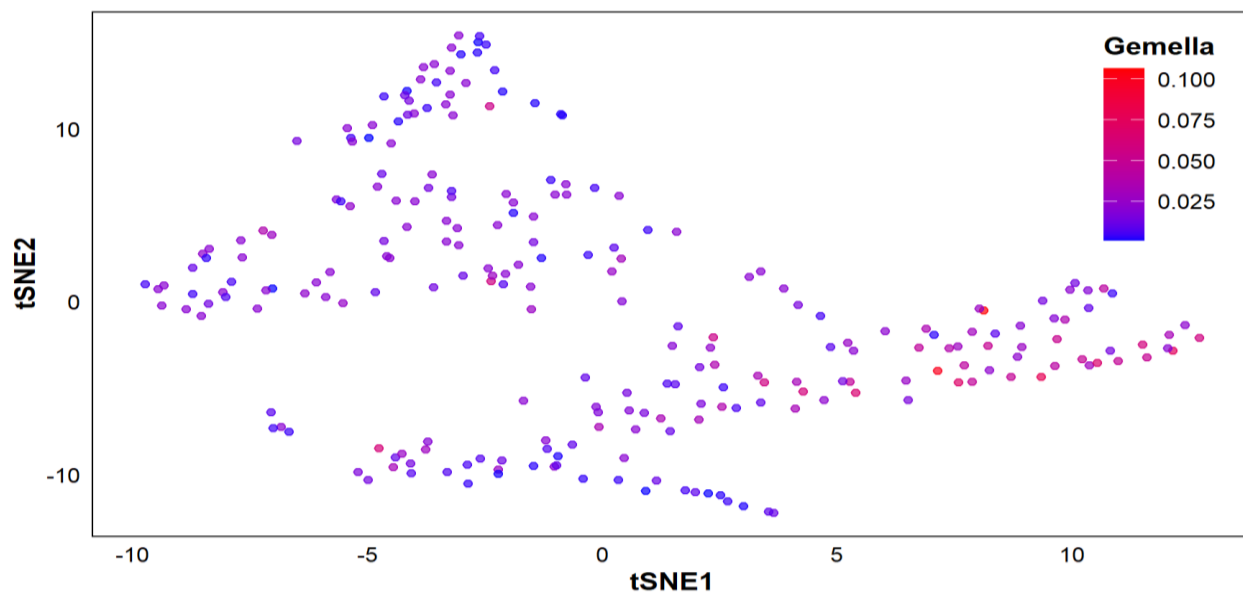


351

352 **Fig S1b:** Mean and standard error of the relative abundance of  
353 *genus Campylobacter* in orotypes 1 to 4.  $P = 0.236$  by Jonckheere-Terpstra  
354 trend test.

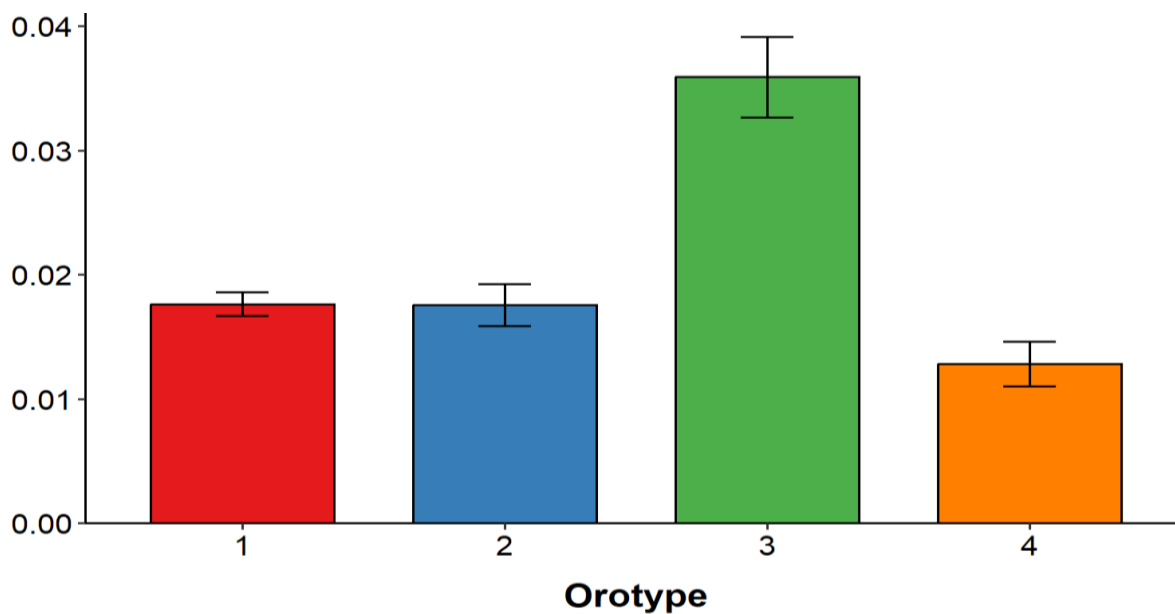
355

356



357

358 **Fig S1c: The t-SNE plot is color-coded by the relative abundance of**  
359 **genus *Gemella*.**



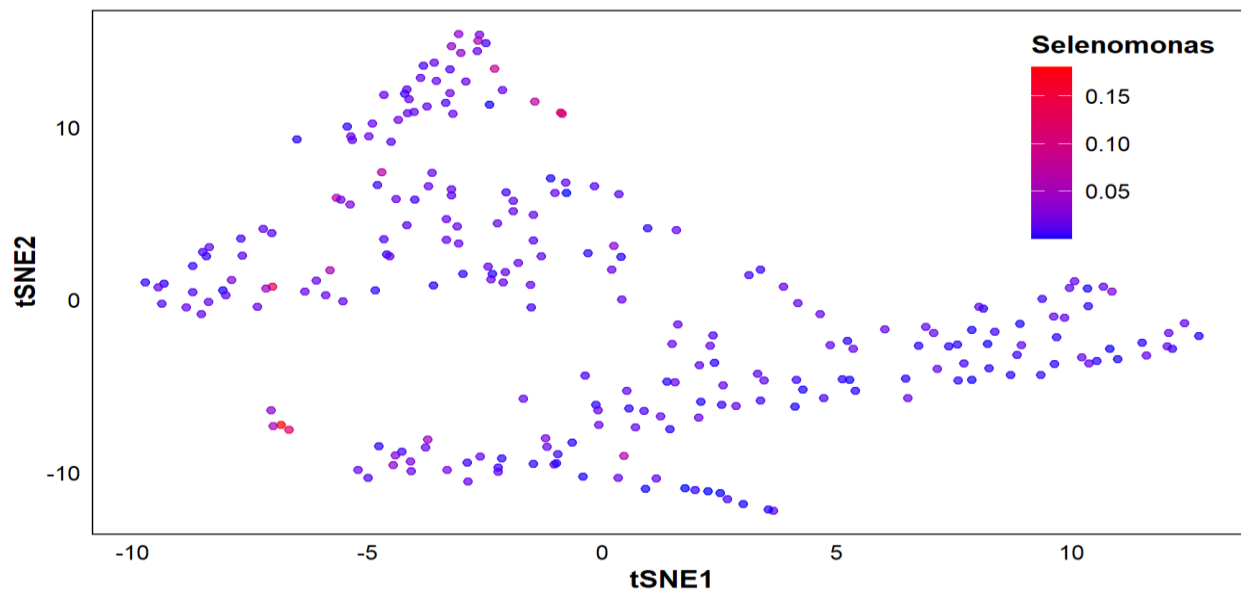
360

361

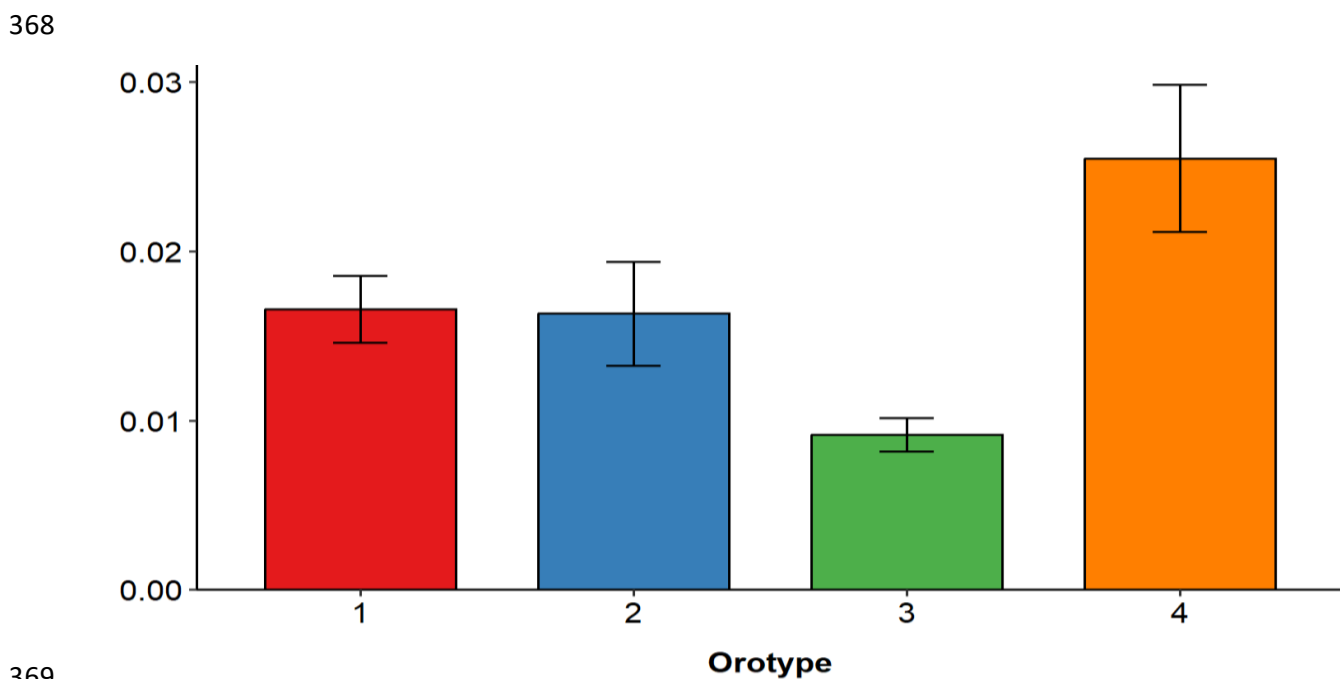
362 **Fig S1d: Mean and standard error of the relative abundance of genus *Gemella***  
363 **in orotypes 1 to 4.  $P = 0.652$  by Jonckheere-Terpstra trend test.**

364



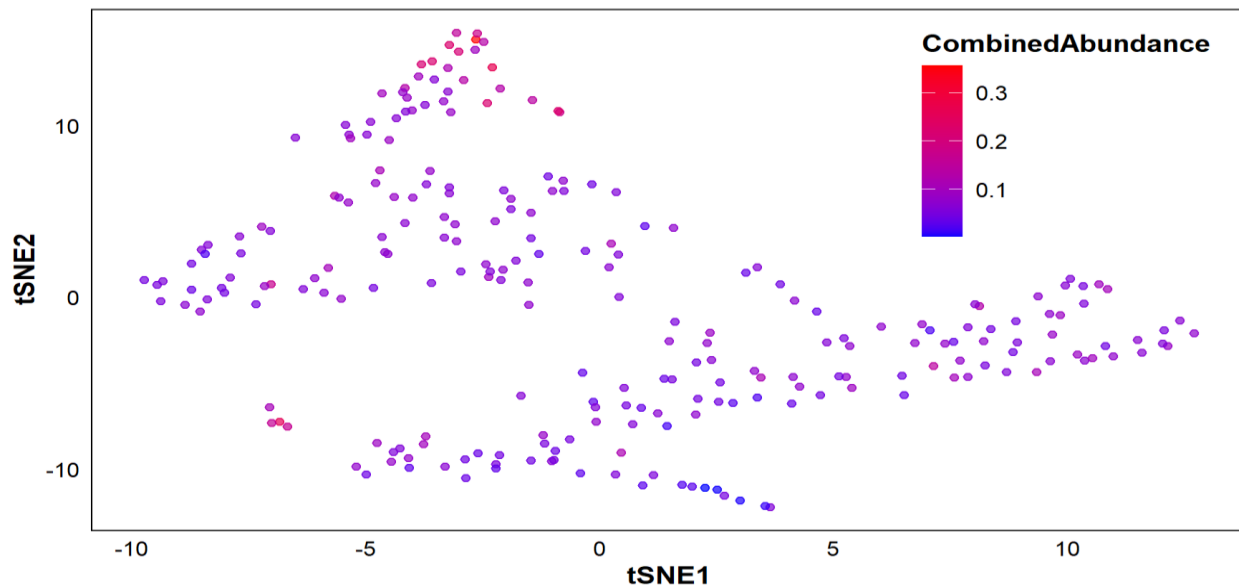


365  
366 **Fig S1e: The t-SNE plot is color-coded by the relative abundance of**  
367 **genus *Selenomonas*.**



369  
370 **Fig S1f: Mean and standard error of the relative abundance of**  
371 **genus *Selenomona* in orotypes 1 to 4.  $P = 0.859$  by Jonckheere-Terpstra trend**  
372 **test.**

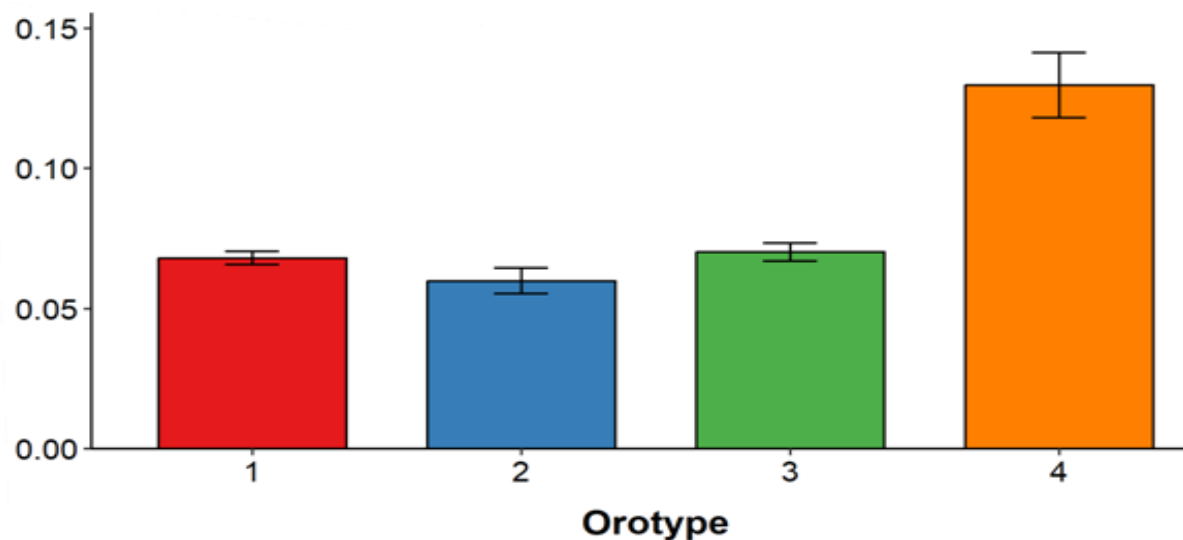
373



374

375 **Fig S1g: The t-SNE plot is color-coded by the relative combine abundance of**  
376 **genus *Treponema*, *Gemella*, *Campylobacter*, *Selenomonas*.**

377



378

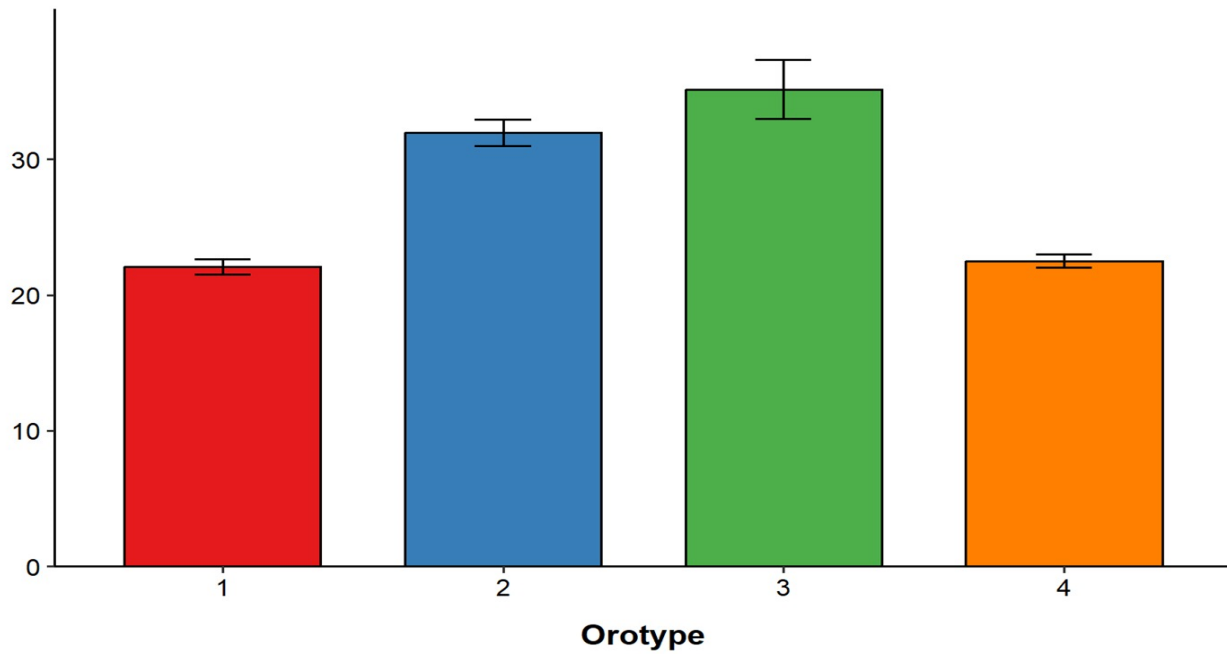
379 **Fig S1h: Mean and standard error of the relative combine abundance of**  
380 **genus *Treponema*, *Gemella*, *Campylobacter*, *Selenomonas* in orotypes 1 to 4. p**  
381 **= 7.198e-05 by Jonckheere-Terpstra trend test.**

382

383

384

385



386

387 **Fig S2: Mean and standard error of the Influenza mortality rates in orotypes**  
388 **1 to 4.  $p = 4e - 04$  by Jonckheere-Terpstra trend test.**

389

390 **Supplementary Table 1. Generalized linear model (GLM) to predict the COVID-19**  
391 **mortality rates with 15 oral bacteria**

392

<b>Genera</b>	<b>P-value</b>	<b>Relative abundance (%)<sup>a</sup></b>
<b>Streptococcus</b>	0.401	21.34
<b>Fusobacterium</b>	0.354	11.18
<b>Veillonella</b>	0.45	8.76
<b>Prevotella</b>	0.439	11.84
<b>Hemophilus</b>	0.644	3.86
<b>Rothia&lt;high G+CGram-positivebacteria&gt;</b>	0.977	5.09
<b>Actinomyces</b>	0.536	3.67
<b>Leptotrichia</b>	0.829	2.97
<b>Prophyromonas</b>	0.474	3.86
<b>Neisseria</b>	0.742	3.26
<b>Corynebacterium</b>	0.577	2.18
<b>Gemella</b>	0.138	2.08
<b>Campylobacter</b>	0.136	1.49
<b>Selenomonas</b>	0.14	1.63
<b>Treponema</b>	0.125	2.35

393 <sup>a</sup>Average relative abundance in 244 healthy subjects in eight countries

394

395

396 **Supplementary Table 2: Most abundance genera in each orotype**

397

---

orotype	Top 5 Genera
1	<i>Streptococcus, Prevotella, Veillonella, Fusobacterium, Haemophilus</i>
2	<i>Streptococcus, Fusobacterium, Prevotella, Rothia (high G+C Gram-positive bacteria), Veillonella</i>
3	<i>Streptococcus, Fusobacterium, Prevotella, Veillonella, Actinomyces</i>
4	<i>Streptococcus, Veillonella, Prevotella, Fusobacterium, Megasphaera</i>

---

398

399

400 **Supplementary Table 3. The mean relative abundances of 15 most prevalent**  
 401 **genera for each orotype**

402

Genus	Orotype 1	Orotype 2	Orotype 3	Orotype 4
<i>Streptococcus</i>	18.00%	35.33%	42.79%	5.60%
<i>Fusobacterium</i>	13.91%	5.12%	4.22%	46.79%
<i>Veillonella</i>	6.99%	19.50%	7.53%	5.76%
<i>Prevotella</i>	9.86%	26.60%	10.87%	6.69%
<i>Haemophilus</i>	4.51%	3.25%	10.03%	3.29%
<i>Rothia</i> <high G+C Gram-positive bacteria>	6.61%	4.24%	10.60%	2.77%
<i>Actinomyces</i>	10.66%	2.07%	1.58%	3.56%
<i>Leptotrichia</i>	5.64%	3.25%	2.56%	2.69%
<i>Porphyromonas</i>	5.04%	3.13%	5.37%	8.68%
<i>Neisseria</i>	5.00%	2.66%	7.17%	2.60%
<i>Corynebacterium</i>	5.43%	1.53%	1.38%	1.97%
<i>Gemella</i>	2.69%	2.14%	4.58%	1.59%
<i>Campylobacter</i>	2.14%	1.12%	0.98%	4.64%
<i>Selenomonas</i>	2.42%	1.90%	1.17%	3.03%
<i>Treponema</i>	3.12%	1.86%	2.24%	6.78%

403

404

405

## List of legend

406

### Supplementary information of legend

407

**Fig S1:** (a) The t-SNE plot is color-coded by the relative abundance of

408

genus *Campylobacter*. (b) Mean and standard error of the relative abundance of

409

genus *Campylobacter* in orotypes 1 to 4.  $P = 0.236$  by Jonckheere-Terpstra trend

410

test. (c)The t-SNE plot is color-coded by the relative abundance of genus *Gemella*.

411

(d)Mean and standard error of the relative abundance of genus *Gemella* in orotypes

412

1 to 4.  $P = 0.652$  by Jonckheere-Terpstra trend test. (e)The t-SNE plot is color-

413

coded by the relative abundance of genus *Selenomonas*. (f)Mean and standard error

414

of the relative abundance of genus *Selenomona* in orotypes 1 to 4.  $P = 0.859$  by

415

Jonckheere-Terpstra trend test. (g)The t-SNE plot is color-coded by the relative

416

combine abundance of genus *Treponema*, *Gemella*, *Campylobacter*, *Selenomonas*.

417

(h)Mean and standard error of the relative combine abundance of

418

genus *Treponema*, *Gemella*, *Campylobacter*, *Selenomonas* in orotypes 1 to 4.  $p =$

419

$7.198e-05$  by Jonckheere-Terpstra trend test.

420

**Fig S2:** Mean and standard error of the Influenza mortality rates in orotypes 1 to

421

4.  $p = 4e - 04$  by Jonckheere-Terpstra trend test

422

**Supplementary Table 1:** Generalized linear model (GLM) to predict the COVID-

423

19 mortality rates with 15 oral bacteria

424 **Supplementary Table 2:** Most abundance genera in each orotype

425 **Supplementary Table 3:** The mean relative abundances of 15 most prevalent

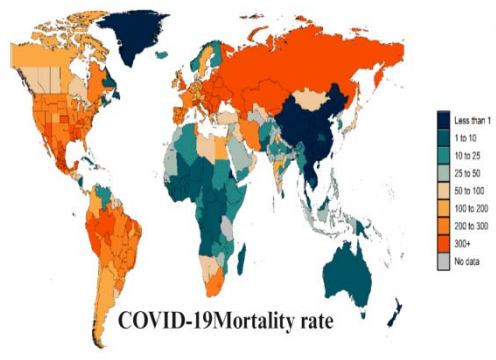
426 genera for each orotype



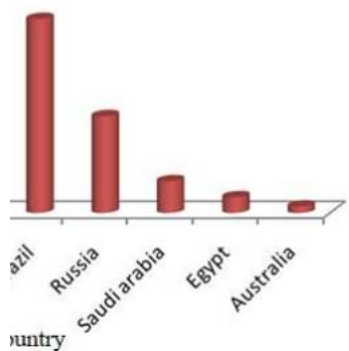
# Question

# Methods

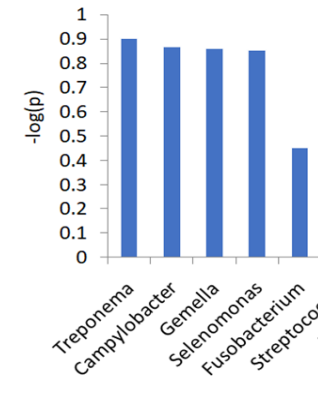
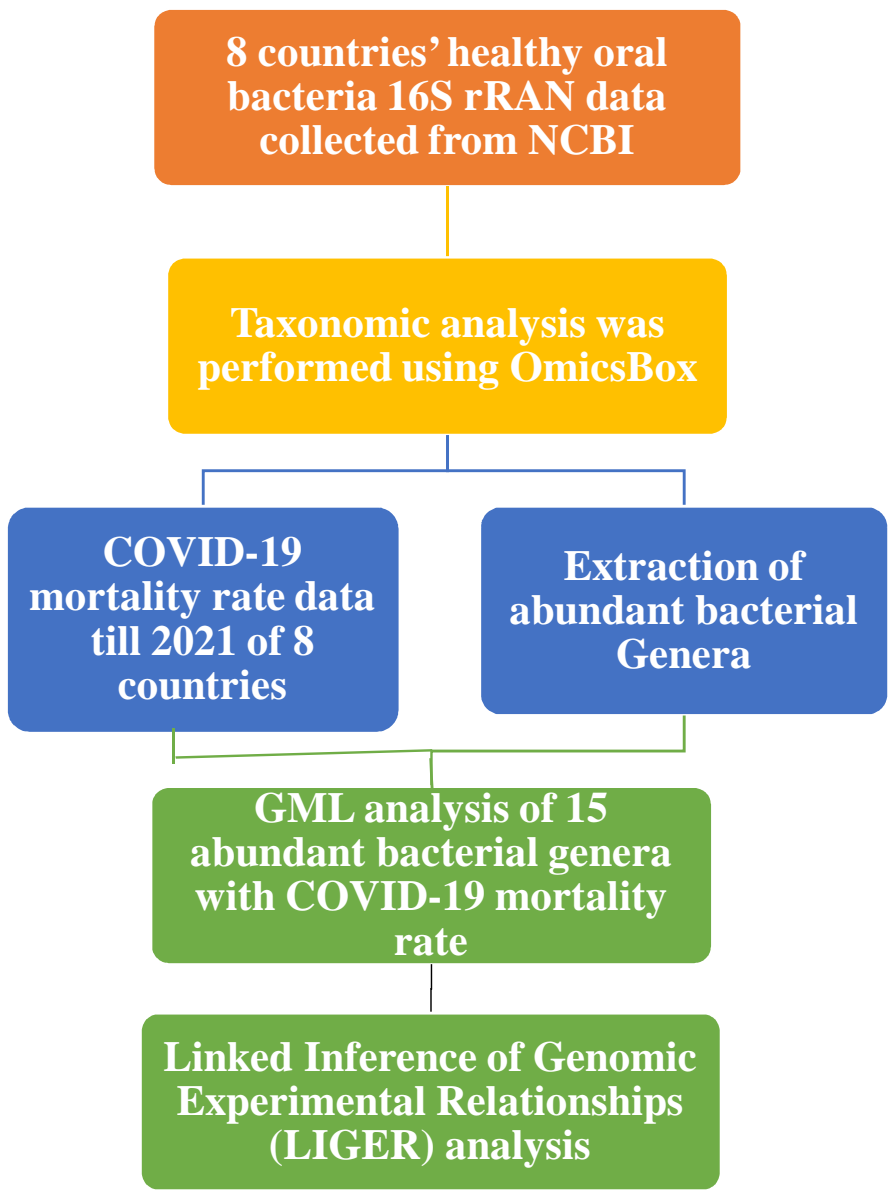
# Results



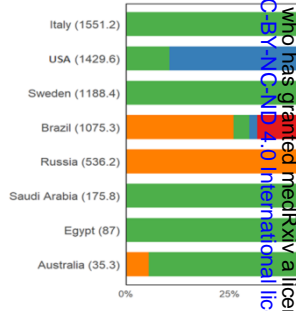
Do bacteria influence COVID-19 mortality rates across the globe?



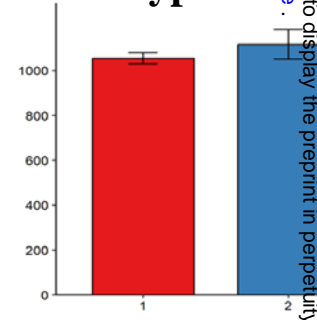
Five countries' Covid-19 mortality rates



Four H<sub>2</sub>S producing CO<sub>2</sub> producing bacterial genera



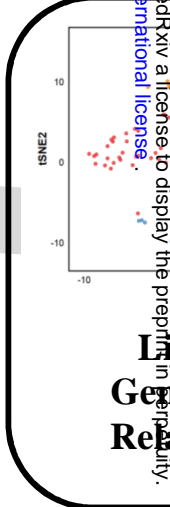
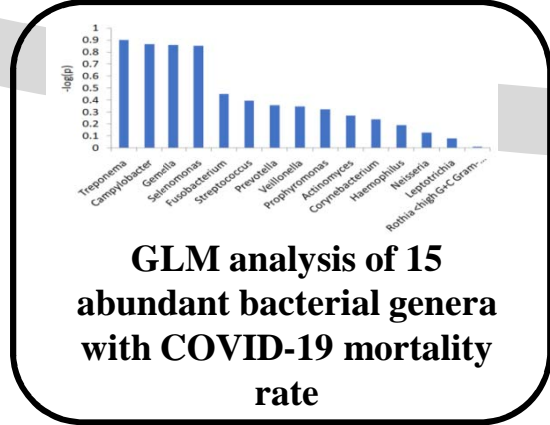
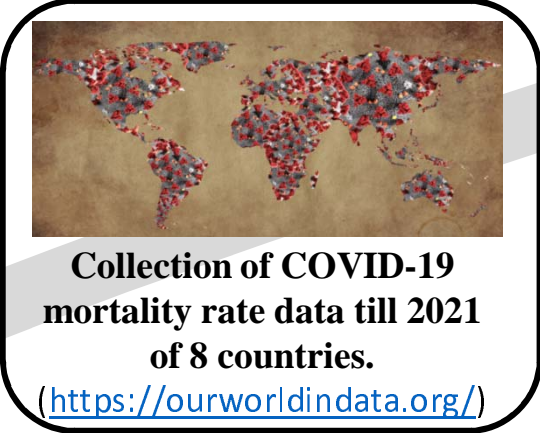
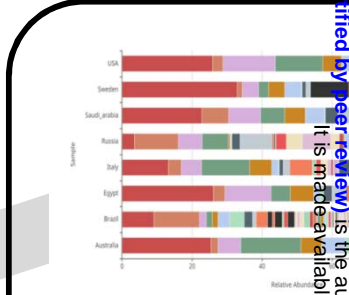
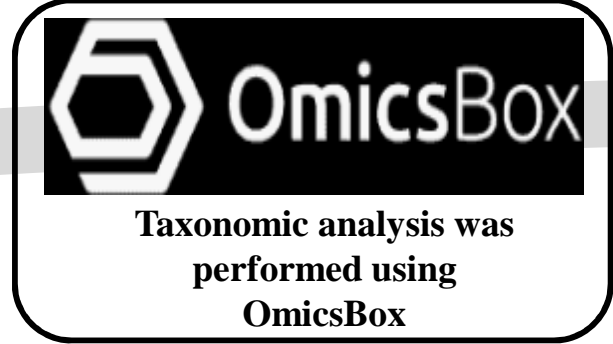
Four orotypes compared



Covid-19 mortality

medRxiv preprint doi: <https://doi.org/10.1101/2024.08.07.24311606>; this version posted August 8, 2024. The copyright holder for this preprint (which was not certified by peer review) is the author/funder, who has granted medRxiv a license to display the preprint in perpetuity. It is made available under a CC-BY-NC-ND 4.0 International license.

logy for this  
 (a) Healthy  
 was obtained  
 Center for  
 ation (NCBI).  
 processed and  
 Box software.  
 lant bacterial  
 . (d) COVID-  
 ta from Our  
 corporated (e)  
 (Generalized  
 ed to analyze  
 n the 15 most  
 d COVID-19  
 ized technique  
 ally used for  
 cell RNA  
 s applied to  
 obiota of 244  
 o four distinct  
 es".



medRxiv preprint doi: <https://doi.org/10.1101/2024.08.07.24311606>; this version posted August 8, 2024. The copyright holder for this preprint (which was not certified by peer review) is the author/funder, who has granted medRxiv a license to display the preprint in perpetuity. It is made available under a CC-BY-NC-ND 4.0 International license.

**Table 1: Eight 16S rRNA-seq datasets from Eight countries and the mortality rates of COVID-19.**

<b>Dataset</b>	<b>City, Country</b>	<b>Accession number</b>	<b>Mortality rate per million<sup>a</sup></b>	<b>The number of samples</b>	<b>Sequencing</b>
<b>1</b>	Australia	PRJDB5153	35.26	18	16S rRNA (V3-V4)
<b>2</b>	Oklahoma, USA	PRJNA292800	1429.6	57	16S rRNA
<b>3</b>	Trento, Italy	PRJNA227796	1551.22	14	16S rRNA
<b>4</b>	Sweden	PRJNA598825	1188.41	12	16S rRNA (V3-V4)
<b>5</b>	Jazan, Saudi arabia	PRJNA267483	175.84	12	16S rRNA
<b>6</b>	Brazil, Sao Paolo, Piracicaba	PRJNA606501	1075.33	104	16S rRNA (V1-3 and V4-5)
<b>7</b>	Egypt	PRJNA384402	86.95	17	16S rRNA
<b>8</b>	Russia, Moscow	PRJNA256234	536.22	10	16S rRNA

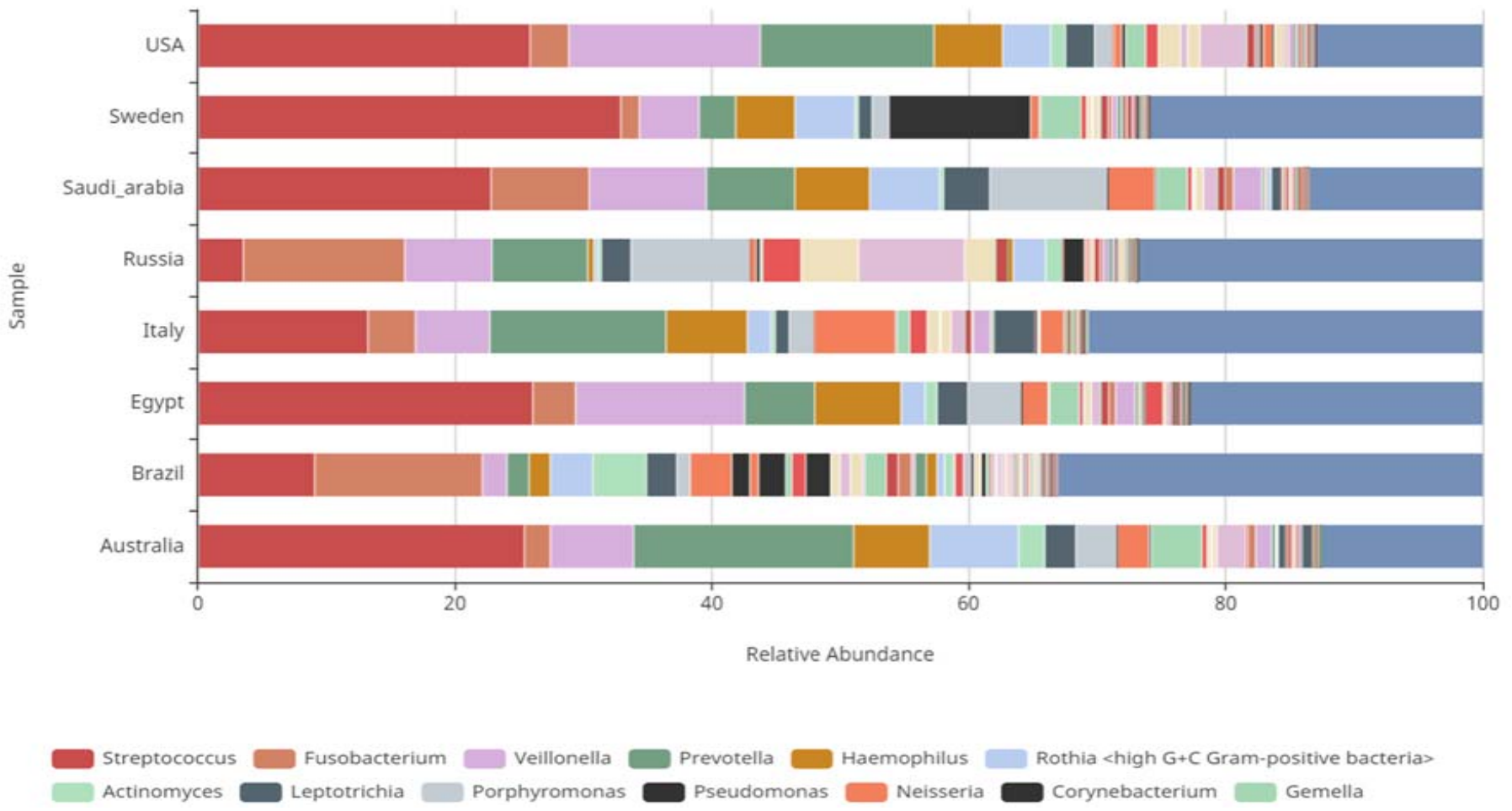


**Fig 2: Genera level abundance of health oral metagenomic**

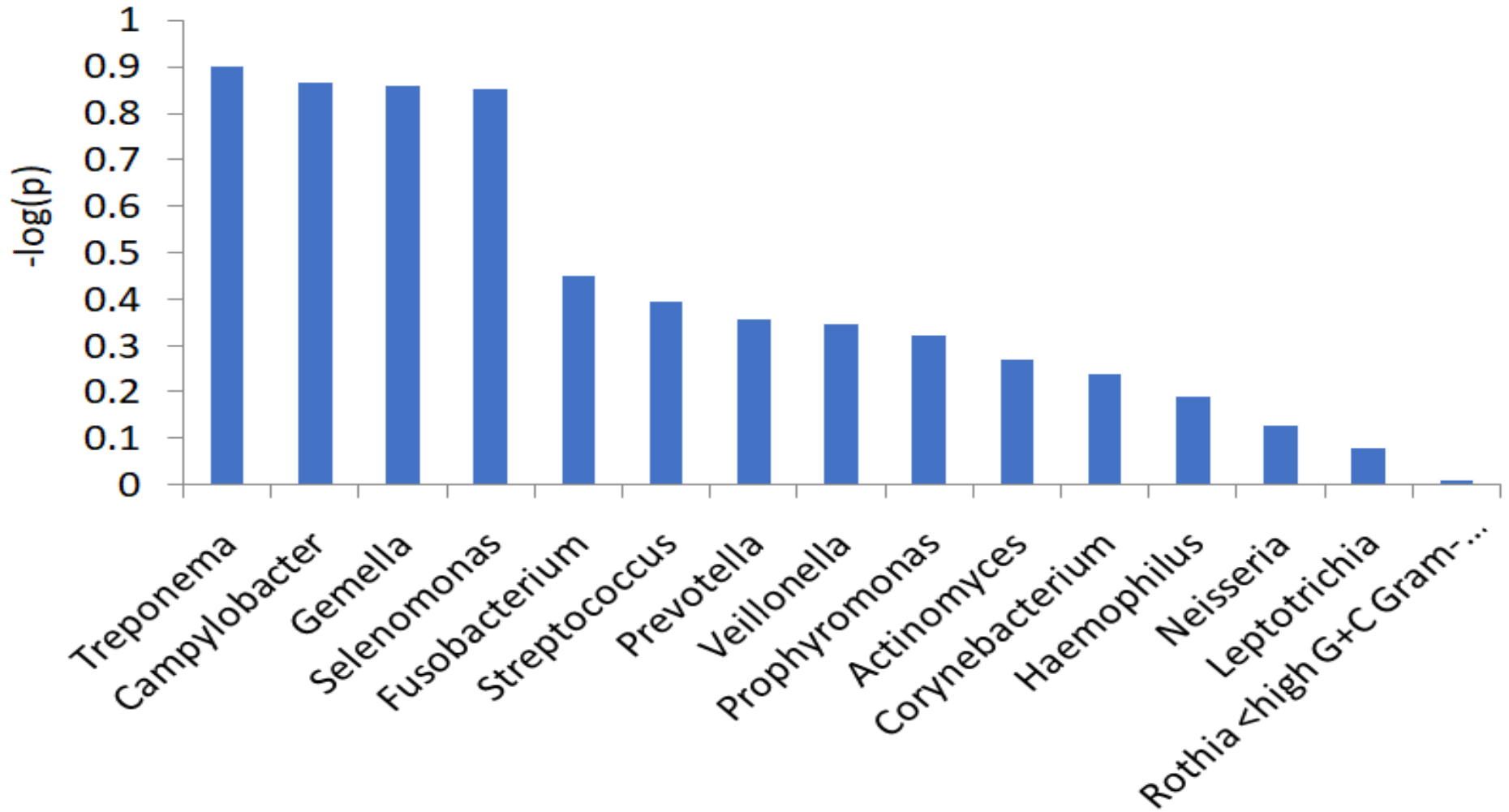


**Fig 3: Plot of p-values of 15 genera in a generalized linear model (GLM) to predict the COVID-19 mortality rates.**

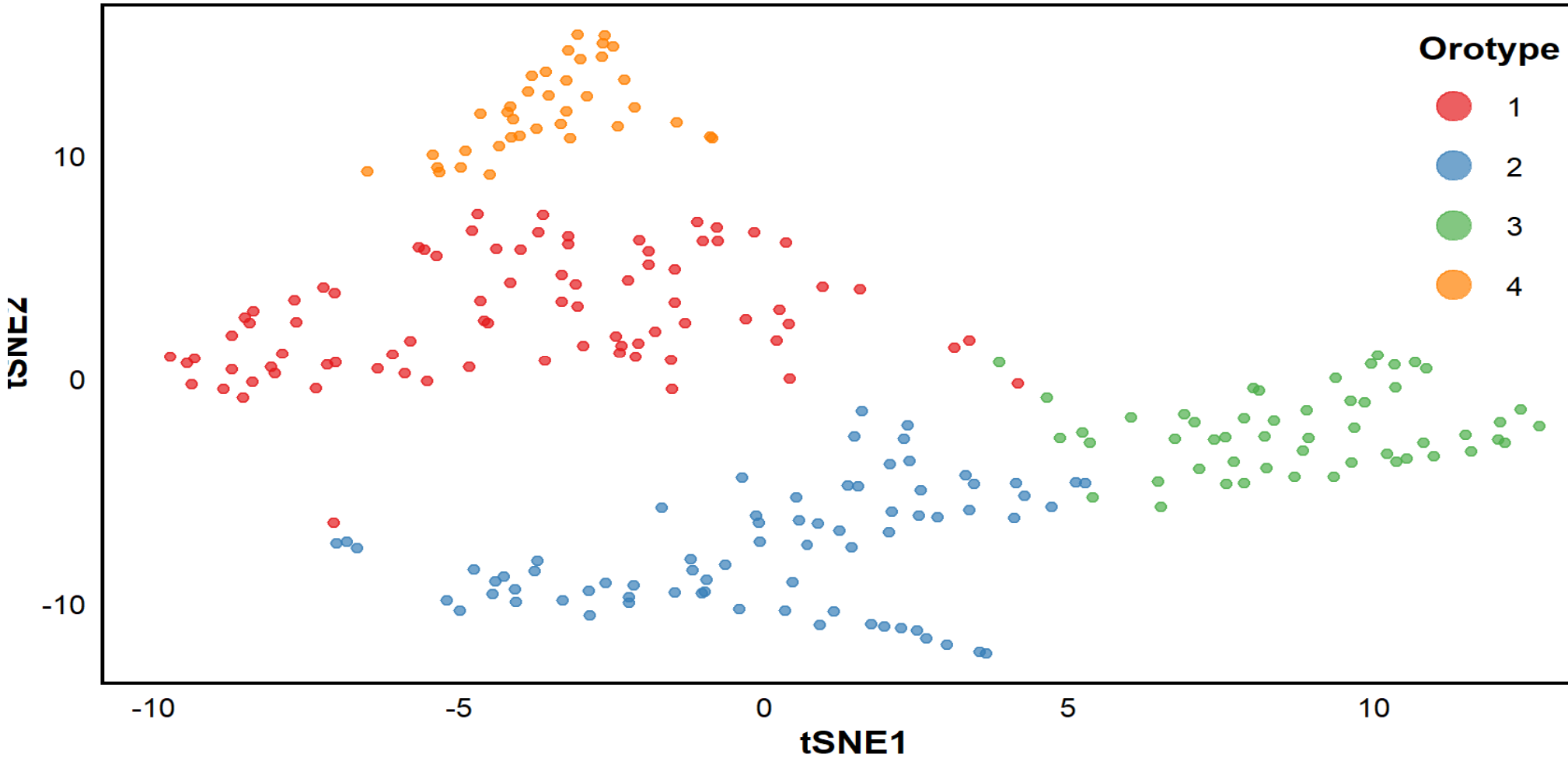


**Fig 4 (a):**Unsupervised clustering of oral microbiota in 244 healthy subjects in ten countries by LIGER generated 4 orotypes. Each subject is plotted with t-SNE and is color-coded by its orotype.

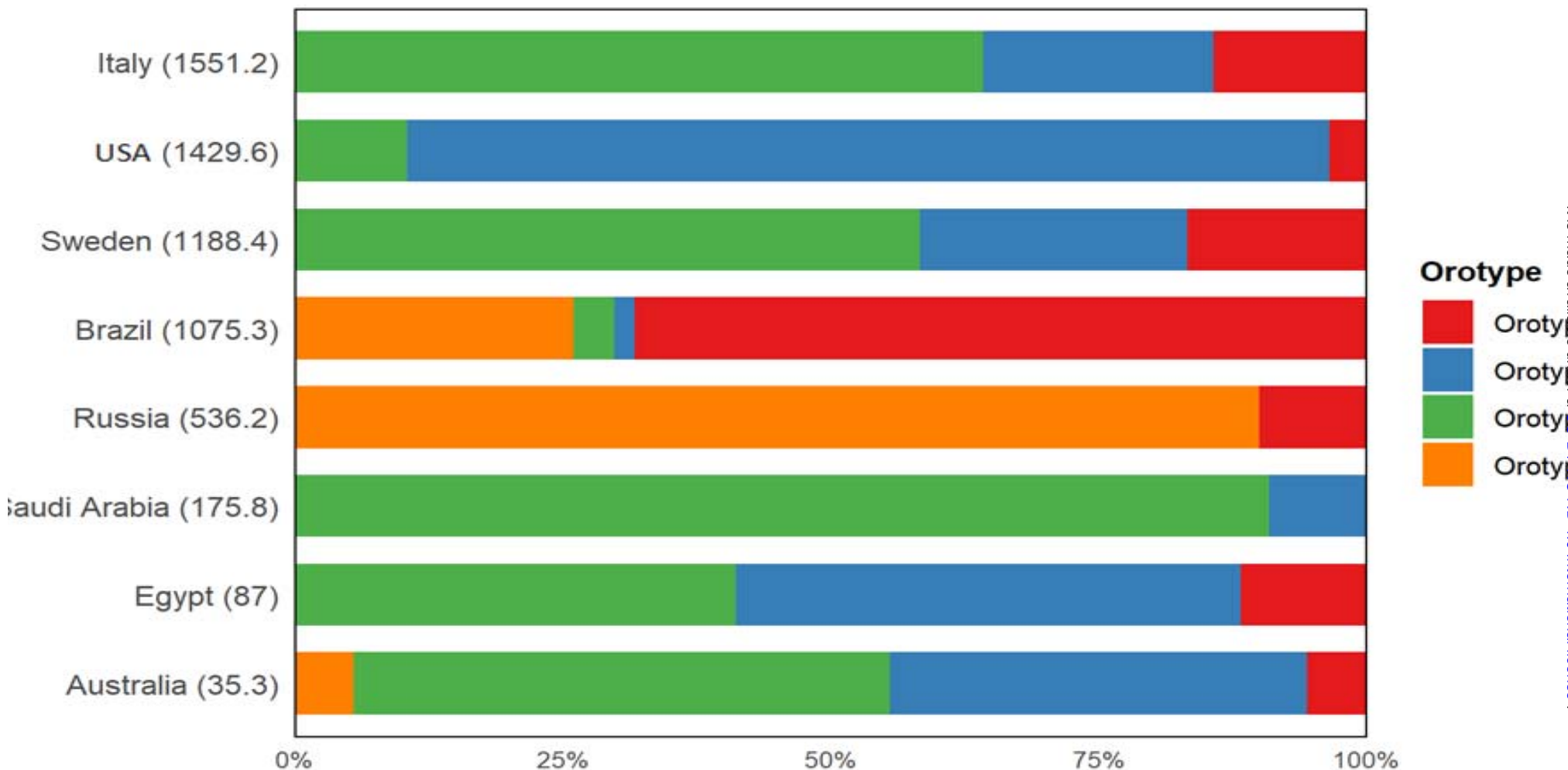


**Fig 4 (b): Fractions of orotypes 1 to 4 in eight countries. eight countries are sorted in descending order of the COVID-19 mortality rates per million, which are indicated in parentheses.**

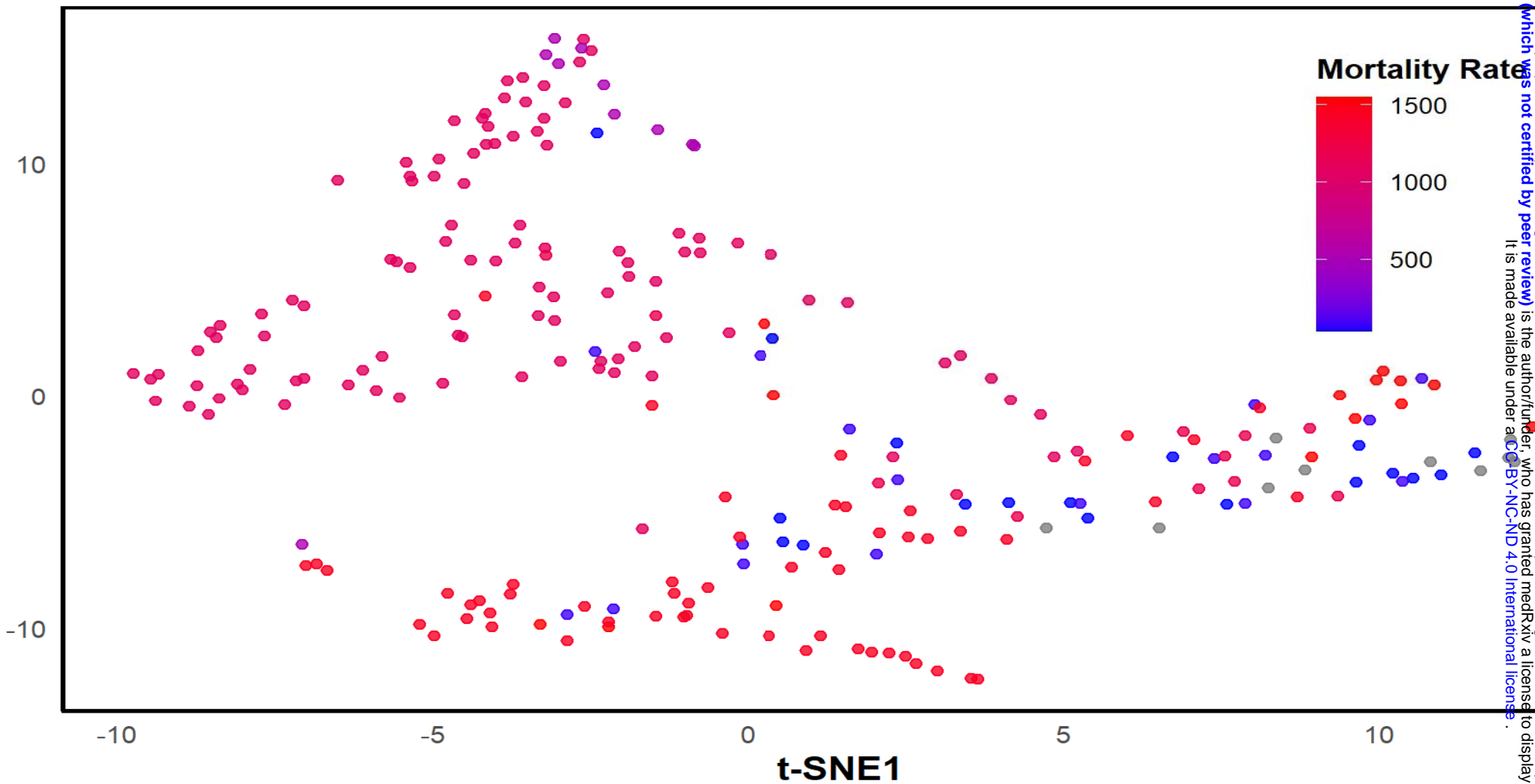


**Fig 4 (c): The t-SNE plot is color-coded by the COVID-19 mortality rates in Eight countries.**



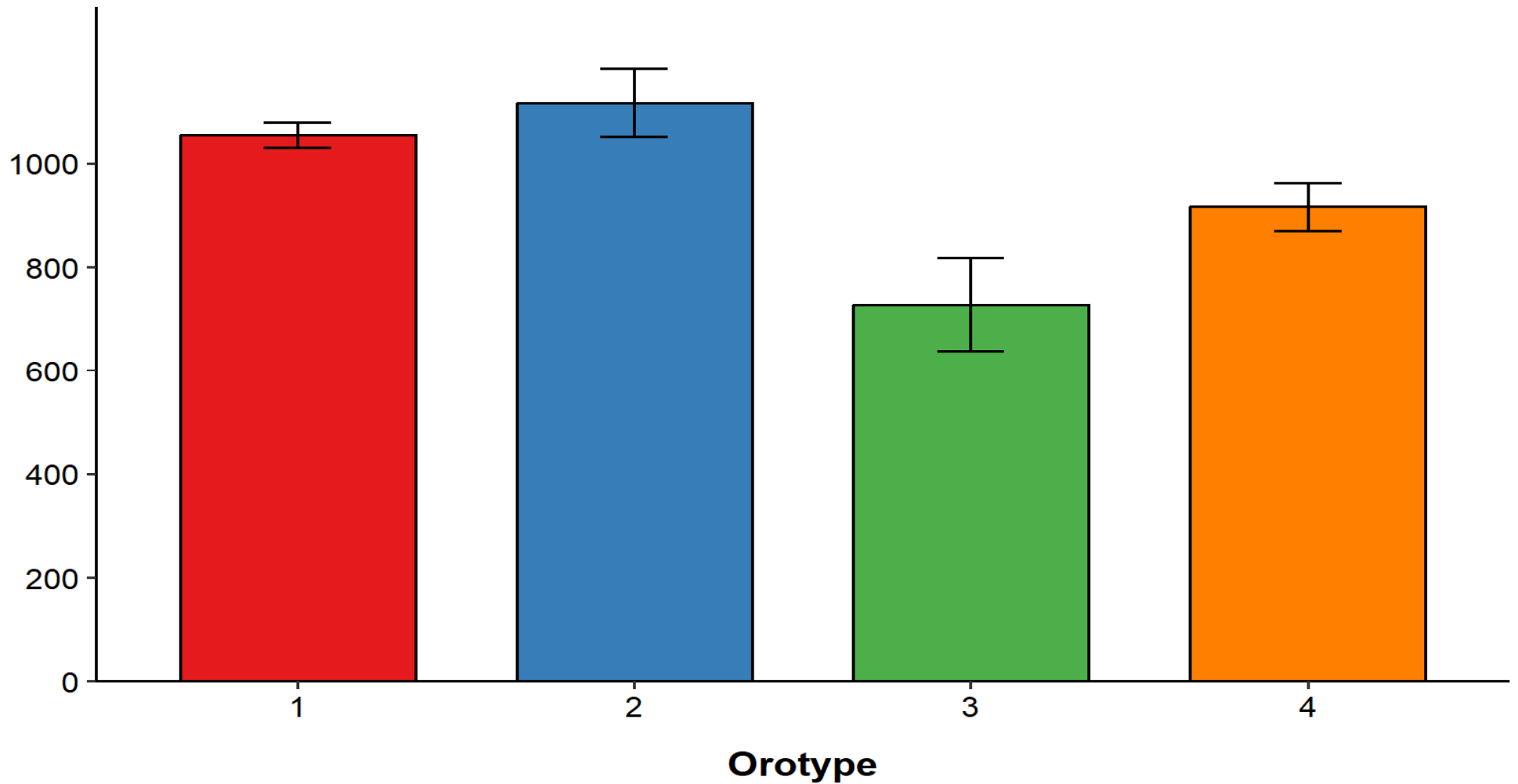


**Fig 4 (d): Mean and standard error of the COVID-19 mortality rates in orotypes 1 to 4.  $p = 0.203$  by Jonckheere-Terpstra trend test.**

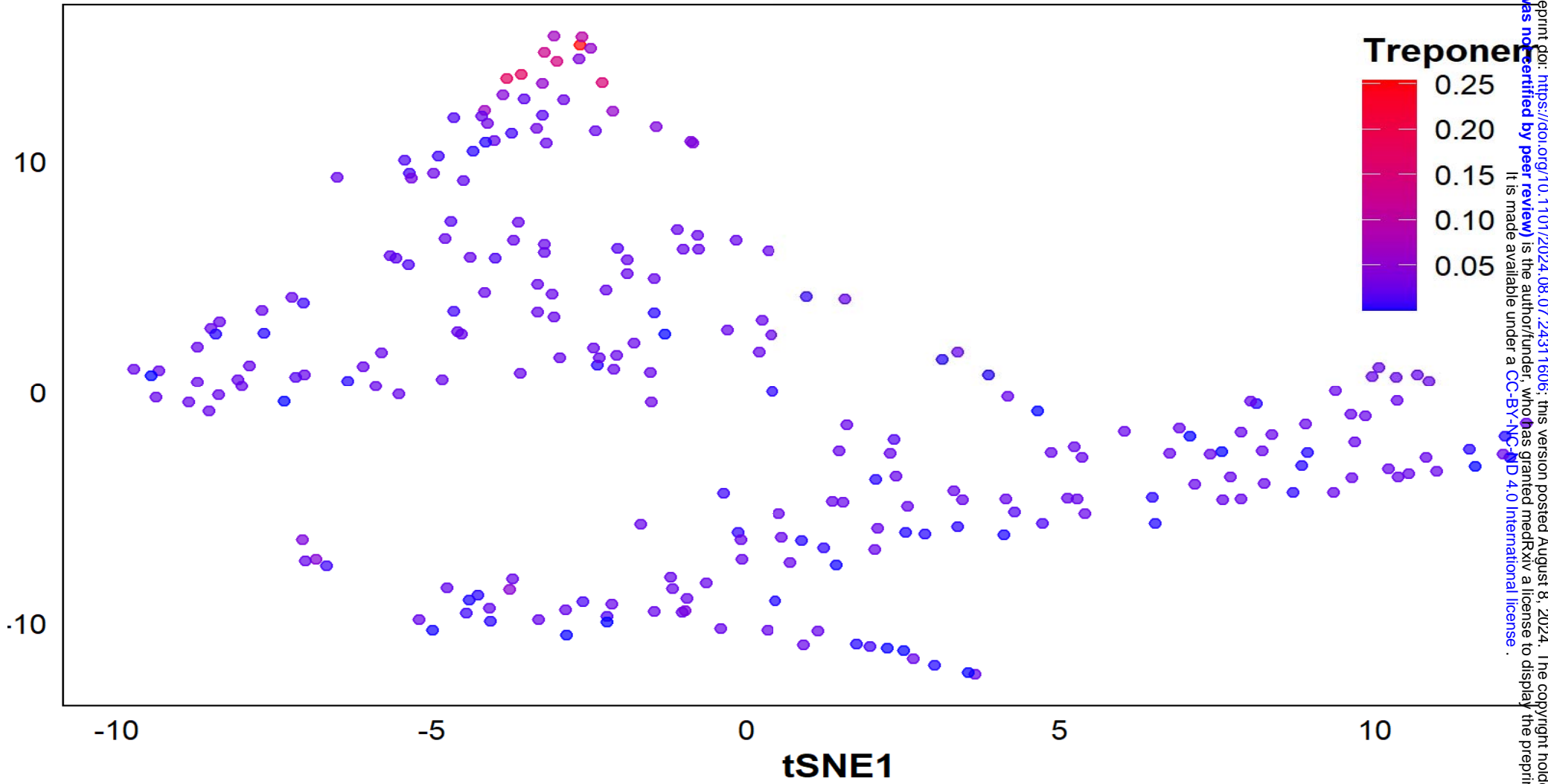


**Fig 4 (e):** The t-SNE plot is color-coded by the relative abundance of genus *Treponema*.

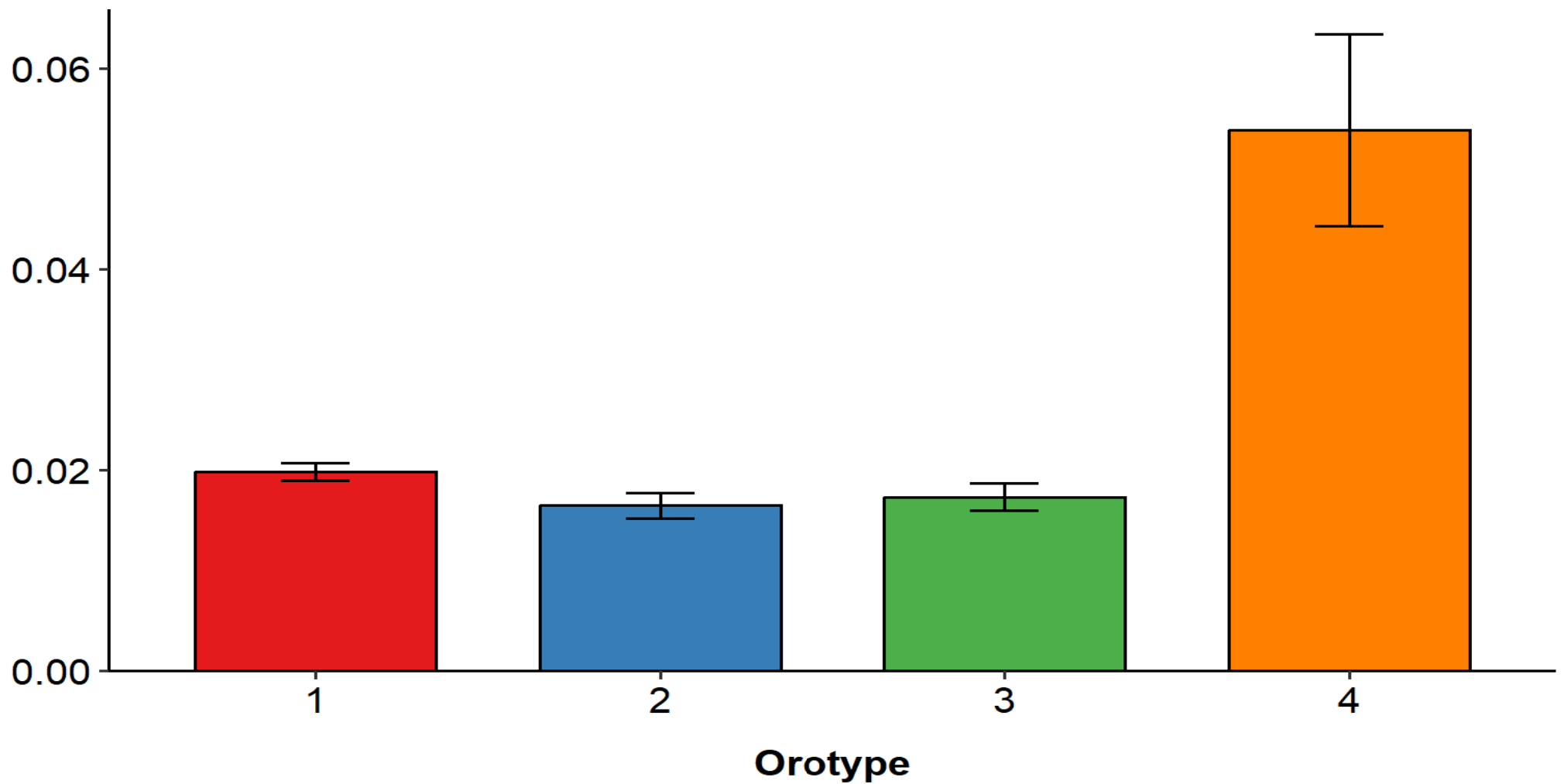


**Fig 4 (f): Mean and standard error of the relative abundance of genus *Treponema* in orotypes 1 to 4.  $P = 0.033$  by Jonckheere-Terpstra trend test.**

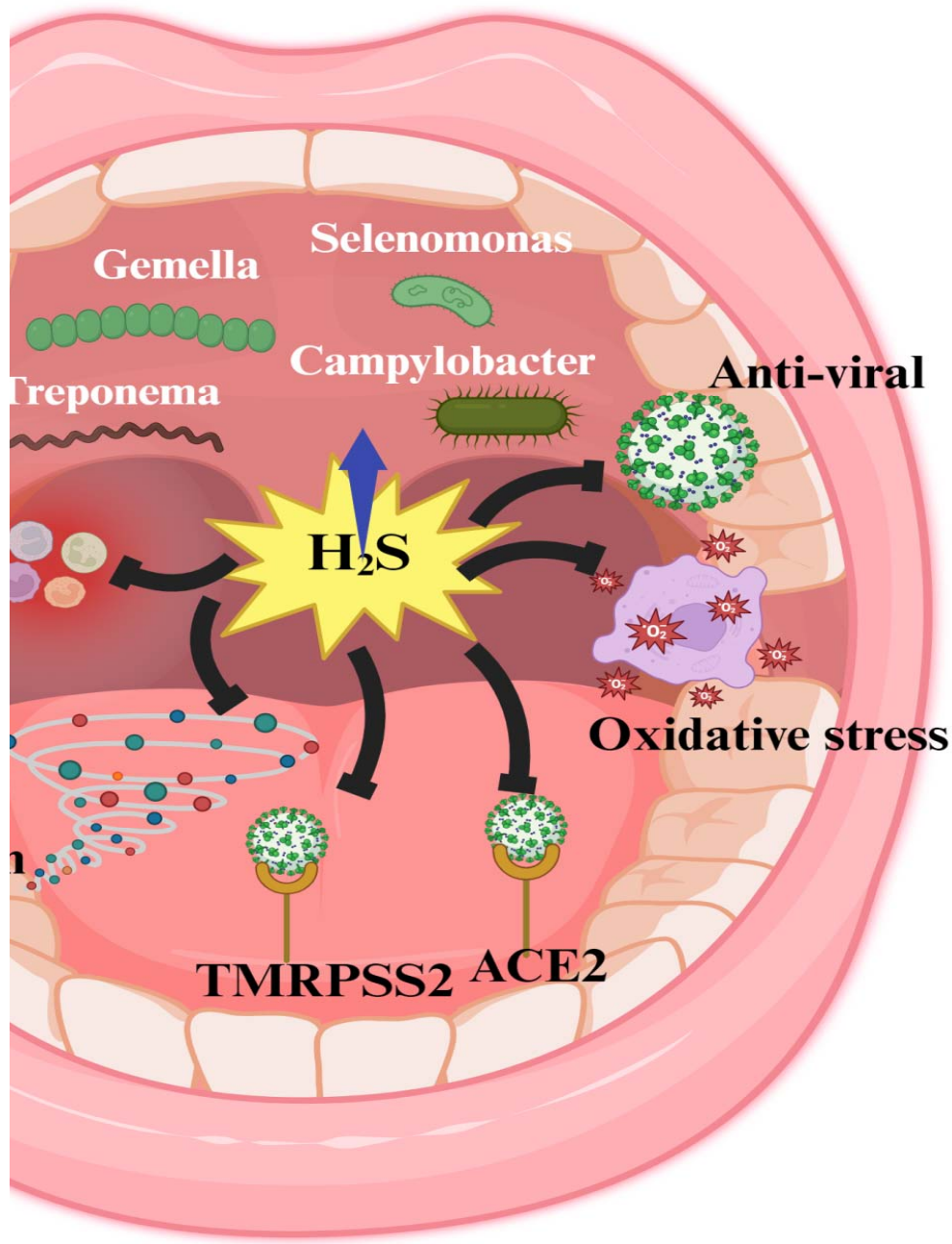


**Fig 5:** Proposed mechanisms of oral hydrogen sulfide (H<sub>2</sub>S) in protecting against viral infection. H<sub>2</sub>S, produced by oral bacteria including Gemella, Campylobacter, and Selenomonas, has multifaceted protective effects against SARS-CoV-2 infection. These effects include: (a) Direct antiviral activity, (b) Modulation of viral entry by altering ACE2 and TMPRSS2 receptor expression, (c) Reduction of inflammatory effects and prevention of cytokine storm, and (d) Enhancement of antioxidant defenses in the oral cavity. These mechanisms, previously shown to be protective against RNA viral infections, likely contribute to the protective role of H<sub>2</sub>S-producing oral bacteria in improving COVID-19 outcomes.

# List of legend

ology for this bioinformatics pipeline (a) Healthy oral microbiome data was obtained from the National Information (NCBI). (b) This data was processed and analyzed using OmicsBox software. (c) The most abundant genera were identified. (d) COVID-19 mortality rate data from Our World in Data was incorporated (e) A statistical Linear Model) was used to analyze the relationship between the 15 most abundant genera and COVID-19 mortality rate. A technique called LIGER, typically used for analyzing single-cell RNA sequencing data, was applied to classify 244 healthy individuals into four distinct groups, termed "orotypes".

6S rRNA-seq datasets from Eight countries and the mortality rates of COVID-19.

Relative abundance of health oral metagenomic

Relative values of 15 genera in a generalized linear model (GLM) to predict the COVID-19 mortality rates.

Revised clustering of oral microbiota in 244 healthy subjects in ten countries by LIGER generated 4 orotypes. (a) t-SNE plot with t-SNE and is color-coded by its orotype. (b) Fractions of orotypes 1 to 4 in eight countries. (c) Ranking order of the COVID-19 mortality rates per million, which are indicated in parentheses. (d) The t-SNE plot of COVID-19 mortality rates in Eight countries. (e) Mean and standard error of the COVID-19 mortality rates in Eight countries by Jonckheere-Terpstra trend test. (f) The t-SNE plot is color-coded by the relative abundance of genus *Treponema*. (g) Standard error of the relative abundance of genus *Treponema* in orotypes 1 to 4.  $P = 0.033$  by Jonckheere-Terpstra trend test.

ed mechanisms of oral bacteria-produced hydrogen sulfide (H<sub>2</sub>S) in protecting against SARS-CoV-2 infection. Oral bacteria including Treponema, Gemella, Campylobacter, and Selenomonas, exhibits multifaceted protection against SARS-CoV-2. These include: (a) Direct antiviral activity, (b) Modulation of viral entry by altering ACE2 receptors, (c) Anti-inflammatory effects and prevention of cytokine storm, and (d) Enhancement of antioxidant defense through the Nrf2 pathway. These mechanisms, previously observed in other RNA viral infections, likely contribute to the protective role of H<sub>2</sub>S-producing oral bacteria against severe COVID-19 outcomes.